Current Research in Food Science 9 (2024) 100815

Contents lists available at ScienceDirect

Current Research in Food Science

journal homepage: www.sciencedirect.com/journal/current-research-in-food-science

Anthocyanins-rich cranberry extract attenuates DSS-induced IBD in an intestinal flora independent manner

Jun Wang [a,1], Zhong-Yu Yuan [a,1], Xin-Yu Wang [a], Ji-Xiao Zhu [c], Wei-Feng Huang [d,**], Guang-Hui Xu [b,***], Li-Tao Yi [a,e,f,*]

[a] Department of Chemical and Pharmaceutical Engineering, College of Chemical Engineering, Huaqiao University, Xiamen, 361021, Fujian province, PR China
[b] Xiamen Medicine Research Institute, Xiamen, 361008, Fujian province, PR China
[c] Research Center of Traditional Chinese Medicine Resources and Ethnic Medicine, Jiangxi University of Chinese Medicine, Nanchang, Jiangxi, 330004, PR China
[d] Department of Gastroenterology and Hepatology, The First Affiliated Hospital of Xiamen University, Xiamen University, Xiamen, 361003, Fujian province, PR China
[e] Institute of Pharmaceutical Engineering, Huaqiao University, Xiamen, 361021, Fujian province, PR China
[f] Fujian Provincial Key Laboratory of Biochemical Technology, Huaqiao University, Xiamen, 361021, Fujian province, PR China

ARTICLE INFO

Handling Editor: Dr. Quancai Sun

Keywords:
Cranberry
Anthocyanins
Inflammatory bowel disease (IBD)
Ferroptosis
Fecal microbiota transplantation (FMT)

ABSTRACT

Cranberry is abundantly rich in anthocyanins, a type of flavonoid with potent antioxidant properties and the resistance against certain diseases. In this study, anthocyanin-rich cranberry extract was extracted, purified, and its components were analyzed. 92.18 % of anthocyanins was obtained and the total content of anthocyanins was 302.62 mg/g after AB-8 resin purification. Quantification analysis showed that the extract mainly contained cyanidin-3-galactoside, procyanidin B2 and procyanidin B4. Then we explored its effects on dextran sulfate sodium (DSS)-induced inflammatory bowel disease (IBD) in mice. The supplementation of cranberry extract resulted in an alleviation of IBD symptoms, evidenced by improvements in the disease activity index (DAI), restoration of colon length and colonic morphology. Cranberry extract reversed the elevated iron and malondialdehyde (MDA) levels and restored glutathione (GSH) levels in IBD mice. Further analysis revealed that cranberry modulated ferroptosis-associated genes and reduced expression of pro-inflammatory cytokines. Although cranberry influenced the intestinal flora balance by reducing Proteobacteria and *Escherichia-Shigella,* and increasing *Lactobacillus*, as well as enhancing SCFAs content, these effects were not entirely dependent on intestinal flora modulation, as indicated by antibiotic intervention and fecal microbiota transplantation (FMT) experiments. In conclusion, our findings suggest that the beneficial impact of cranberry extract on IBD may primarily involve the regulation of colonic ferroptosis, independent of significant alterations in intestinal flora.

1. Introduction

Inflammatory bowel disease (IBD), encompassing conditions such as Crohn's disease and ulcerative colitis, represents a significant public health concern due to its rising global prevalence and substantial impact on patients' quality of life. Characterized by chronic inflammation of the gastrointestinal tract, IBD manifests in a spectrum of symptoms including abdominal pain, severe diarrhea, fatigue, and weight loss, often leading to debilitating complications (Perler et al., 2019). The pathophysiology of IBD is multifactorial, involving a complex interplay of genetic susceptibility, environmental triggers, and aberrant immunological responses (Ramos and Papadakis, 2019). Despite advances in understanding its pathogenesis, IBD remains a challenging condition to manage, underscoring the need for continued research into novel therapeutic strategies.

Ferroptosis, a recently identified form of regulated cell death characterized by iron-dependent lipid peroxidation, is emerging as a significant factor in the pathophysiology of IBD (Xu et al., 2021). This distinct mode of cell death diverges from apoptosis and necrosis in its

* Corresponding author. Department of Chemical and Pharmaceutical Engineering, College of Chemical Engineering, Huaqiao University, Xiamen, 361021, Fujian province, PR China.
** Corresponding author.
*** Corresponding author.
E-mail addresses: 2749489590@qq.com (J. Wang), 2717769010@qq.com (Z.-Y. Yuan), 3402283675@qq.com (X.-Y. Wang), zhujx81@sina.com (J.-X. Zhu), hwf0625@xmu.edu.cn (W.-F. Huang), xghcxm@163.com (G.-H. Xu), litaoyi@hqu.edu.cn (L.-T. Yi).
[1] These authors contributed equally to the work.

https://doi.org/10.1016/j.crfs.2024.100815
Received 17 April 2024; Received in revised form 25 June 2024; Accepted 20 July 2024
Available online 23 July 2024

List of abbreviation

CAT	catalase
DAI	disease activity index
DAPI	4,6-diamidino-2-phenylindole
DSS	dextran sulfate sodium
FMT	fecal microbiota transplantation
FWHM	Full width at half maximum
GAPDH	Glyceraldehyde-3-phosphate dehydrogenase
GPX4	Glutathione Peroxidase 4
GSH	glutathione
H&E	Hematoxylin and Eosin
HO-1	heme oxygenase 1
IBD	Inflammatory bowel disease
IL-1β	interleukin-1 beta
IL-6	interleukin-6
MDA	malondialdehyde
MDI	microbial dysbiosis index
LC-MS	Liquid Chromatograph Mass Spectrometer
OCT	optimal cutting temperature compound
PAS	Periodic Acid-Schiff
PBS	Phosphate Buffered Saline
ROS	reactive oxygen species
SCFAs	short-chain fatty acids
SLC7A11	Solute Carrier Family 7 Member 11
SOD	superoxide dismutase
TBS	Tris Buffered Saline
TNF-α	tumor necrosis factor-alpha
ZO-1	zonula occludens-1

mechanism and biological implications. Crucially, ferroptosis has been implicated in exacerbating inflammatory processes within the gut, contributing to the tissue damage observed in IBD. Current research suggests a complex interaction between ferroptosis and gut health, where the dysregulation of iron metabolism and oxidative stress plays a pivotal role in the inflammatory cascade (Ocansey et al., 2023; Wu et al., 2023).

Cranberries, long revered for their healthy properties, have a rich history of use in treating a variety of ailments, evolving from folk remedies to being the focus of contemporary scientific research. Historically utilized by Native Americans for wound healing and as a general health tonic. Recent literatures have expanded the scope of cranberry health benefits, highlighting their rich composition of phytochemicals, including anthocyanidins, flavonoids, and phenolic acids (Glisan et al., 2016; Liu et al., 2021). These compounds confer significant anti-inflammatory properties, making cranberries a potential therapeutic agent in conditions characterized by chronic inflammation. For example, recent clinical study showed that daily cranberry consumption could improve vascular function in healthy individuals (Heiss et al., 2022). Cranberry consumption could enhance the antioxidant status in *Helicobacter pylori* infection subjects (Gao et al., 2021).

In preclinical experiments, cranberry was found to attenuate obesity and improve insulin resistance via inhibition of inflammation and oxidative stress to reverse hyperlipidemia and fatty liver disease (Feldman et al., 2022). It exerted a hepaprotective role in acute and subacute hepatotoxicity in rats induced by carbon tetrachloride (Sergazy et al., 2023). Cranberry promoted high-density lipoprotein, induced the oxidation of low-density lipoprotein to alleviate heart damage (Salmasi et al., 2023). While the protective effects of anthocyanins and cranberry against ulcerative Colitis have been documented (Cai et al., 2019; Wu et al., 2020), the mechanisms underlying these effects, particularly the role of ferroptosis and the influence on intestinal flora, remain insufficiently explored. The novelty of this study lies in its focus on the specific mechanism of ferroptosis regulation by anthocyanin-rich cranberry extract and its independence from gut microbiota modulation in alleviating dextran sulfate sodium (DSS)-induced IBD symptoms. By conducting antibiotic intervention and fecal microbiota transplantation (FMT) experiments, we aim to delineate whether the therapeutic effects of cranberry extract are primarily mediated through direct modulation of colonic ferroptosis rather than alterations in intestinal flora.

Therefore, given the emerging role of ferroptosis in IBD and the anti-inflammatory properties of cranberries, this study aims to investigate the therapeutic potential of anthocyanin-rich cranberry extract in IBD mouse model. Specifically, we hypothesize that cranberry extract alleviates IBD symptoms primarily through the regulation of colonic ferroptosis, independent of significant alterations in intestinal flora. To test this hypothesis, we conducted antibiotic intervention and FMT experiments to elucidate the underlying mechanisms of cranberry on IBD.

2. Materials and methods

2.1. Extraction of anthocyanin from cranberry

In this study, ultrasound-assisted extraction methodology, refined through preliminary experiments, was employed for the isolation of anthocyanins from cranberry. The cranberries (Collected in October 2023 in Fuyuan of Heilongjiang Province of China) were first homogenized using a mechanical juicer, followed by incubation in a solvent mixture composed of 60% ethanol containing 0.1 M HCl, in a ratio of 6:1 (v/v). This mixture was then exposed to ultrasound-assisted extraction for a duration of 60 min, utilizing an ultrasonic power setting of 140 W and a controlled temperature of 30 °C. Post-extraction, the solution underwent filtration, and the resulting filtrates were concentrated under reduced pressure. This step led to the production of a dark red viscous substance, referred to as the crude anthocyanin extracts. Quantification of the extraction yield and the anthocyanin content within the crude extracts was conducted using the pH differential method, providing a measure of the extraction efficiency.

2.2. Purification of anthocyanin from crude extracts of cranberry

The crude anthocyanin extracts obtained were first diluted with distilled water in a 1:2 ratio. This diluted mixture then underwent a series of ethyl acetate extractions, performed four times to enhance purity. Subsequently, the aqueous phase of the mixture was re-concentrated. The concentrated extract was then subjected to purification using AB-8 resins. The purification process encompassed a 2-h adsorption phase and a 2-h desorption phase. During these phases, the concentration of the crude extracts was maintained at 0.4 g/mL. The elution process involved 70% ethanol as the eluent, with flow rates set at 1 mL/min for the crude extracts and 2 mL/min for the eluent. Following the elution process, the eluent was concentrated at 40 °C under reduced pressure. The resulting purified cranberry anthocyanins were then subjected to freeze-drying. The anthocyanin content in the final product was quantitatively analyzed using the pH differential method, providing an assessment of the purity and concentration of the anthocyanins.

2.3. pH differential method for anthocyanins measurement

The quantification of the total anthocyanin content was performed utilizing the pH differential method, which was widely recognized for its specificity and sensitivity in determining anthocyanin concentrations. In the first step of this procedure, 1 mL of the extract was diluted to a final

Table 1
Antibody information.

Antibody	Catalog No. and Dilution	Source
Rabbit Occludin	ab216327 (1:100)	Abcam
Rabbit Claudin-1	ab307692 (1:100)	Abcam
Rabbit ZO-1	ab221547 (1:100)	Abcam
Mouse SLC7A11	MA544922 (1:200)	Thermofisher
Rabbit Phospho-Nrf2	PA567520 (1:200)	Thermofisher
Rabbit Ferritin light chain	PA5-119112 (1:200)	Thermofisher
Rabbit Transferrin Receptor	ab269513 (1:100)	Abcam
Rabbit GPX4	ab125066 (1:100)	Abcam

Table 2
Disease activity index score.

Score	Weight loss	Fecal viscosity	Fecal occult blood
0	None	Normal	Negative
1	1–5%	Soft stool	Light blue
2	5–10%	Mucoid stool	Blue
3	>10%	Watery stool	Deongaree

Table 3
Histological scoring criteria.

Score	Pathological range	Inflammatory infiltration	Epithelial cell changes
1	1–25%	Around crypt basis	Goblet cell deficiency
2	26–50%	Mucosal muscle layer	Massive loss of goblet cells
3	51–75%	Mucosal muscle lauyer and	Crypts deficiency
4	76–100%	Submucosa	Massive loss of crypts

volume of 10 mL using two different buffers, separately. For the first dilution, a potassium chloride buffer (0.025 M) was used to adjust the solution to pH 1, a condition that stabilizes anthocyanins in their flavylium cation form. The second dilution was achieved by adjusting the extract to pH 4.5 using a sodium acetate buffer (0.4 M), which promotes the formation of the quinoidal base form of anthocyanins. Following the preparation of these dilutions, the absorbance of each was measured spectrophotometrically at two distinct wavelengths. The absorbance at 510 nm, the λ_max for cyanidin 3-glucoside, and at 700 nm, to correct for any haze and turbidity in the solutions, were both recorded. The total anthocyanin content in the extracts was then calculated, with the results expressed as cyanidin 3-glucoside equivalents per gram of the sample. In these calculations, the molar absorptivity (ε) of cyanidin 3-glucoside, with a value of 26,900, was an essential parameter.

2.4. Quantification of anthocyanins by UPLC

The method of anthocyanins analysis was according to the previous studies (Barnes et al., 2009; Glauser et al., 2016). Quantitative analysis of anthocyanins was performed using fifteen selected standards: Cyanidin-3,5-diglucoside, Cyanidin-3-galactoside, Delphinidin, Procyanidin B4, Cyanidin, Procyanidin B2, Petunidin, Pelargonidin, Peonidin, Malvidin, Rutin, Luteolin, Quercetin, Isorhamnetin, and Kaempferol (Supplementary file 1). These analytes were chosen based on their prevalence in various botanical sources and their significance in nutritional studies. All standards were procured from Sigma-Aldrich (St. Louis, USA). To construct calibration curves, mixed standard solutions were prepared in concentrations ranging from 50 to 2000 ng/mL. Sample preparation involved accurately weighing 100 mg of the dried plant material, followed by dual extractions using 1 mL of a solvent mixture composed of methanol, water, and formic acid (70:30:1, v/v/v). This mixture was selected to optimize the solubilization of anthocyanins. Each sample underwent vigorous vortexing and ultrasonic treatment for 20 min to enhance extraction efficiency. Subsequently, the mixtures were centrifuged at 12,000 rpm for 10 min, and the clear supernatants were filtered through a 0.22 μm nylon membrane filter. Solid-phase extraction (SPE) was conducted using hydrophilic-lipophilic balance (HLB-SPE) columns to purify the extracts. The SPE procedure involved preconditioning the column with 1 mL of methanol followed by 1 mL of deionized water. The anthocyanin-rich supernatant was then percolated through the column, followed by washing with 1 mL of water. Elution of anthocyanins was achieved with 1 mL of methanol containing 5% formic acid. The eluate was collected, dried under a stream of nitrogen, freeze-dried, and reconstituted in 0.2 mL of methanol for further analysis. Chromatographic separation was achieved on a Waters ACQUITY UPLC BEH C18 column (1.8 μm, 2.1 mm × 50 mm) maintained at 40 °C. The mobile phase comprised water and acetonitrile, each containing 0.1% formic acid. The flow rate was set at 0.3 mL/min with an injection volume of 2 μL. The gradient commenced with 95% water and shifted to 70% at 6.0 min, reaching 5% at 7.0 min, and held until 8.1 min, before returning to initial conditions at 10.0 min. Analysis was conducted using an UPLC coupled to an Orbitrap mass spectrometer (Vanquish UPLC and QE MS), optimizing detection and quantification of the targeted analytes. To accurately identify and quantify compounds, we rely on both the mass-to-charge ratio and the

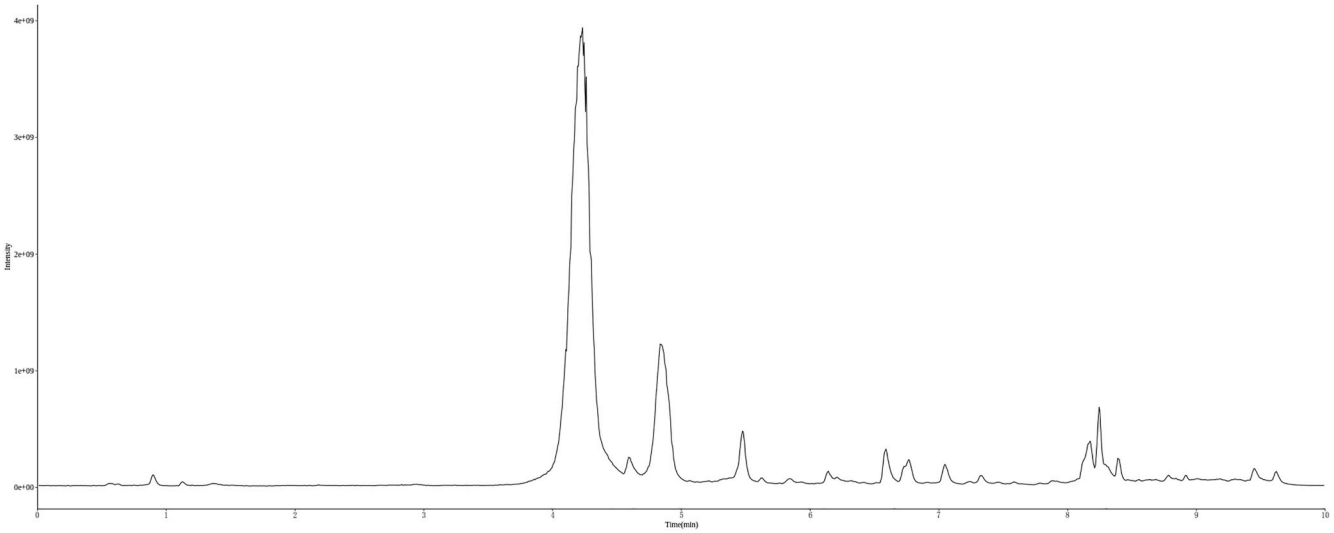

Fig. 1. The total ion flow chromatogram of anthocyanin-rich cranberry.

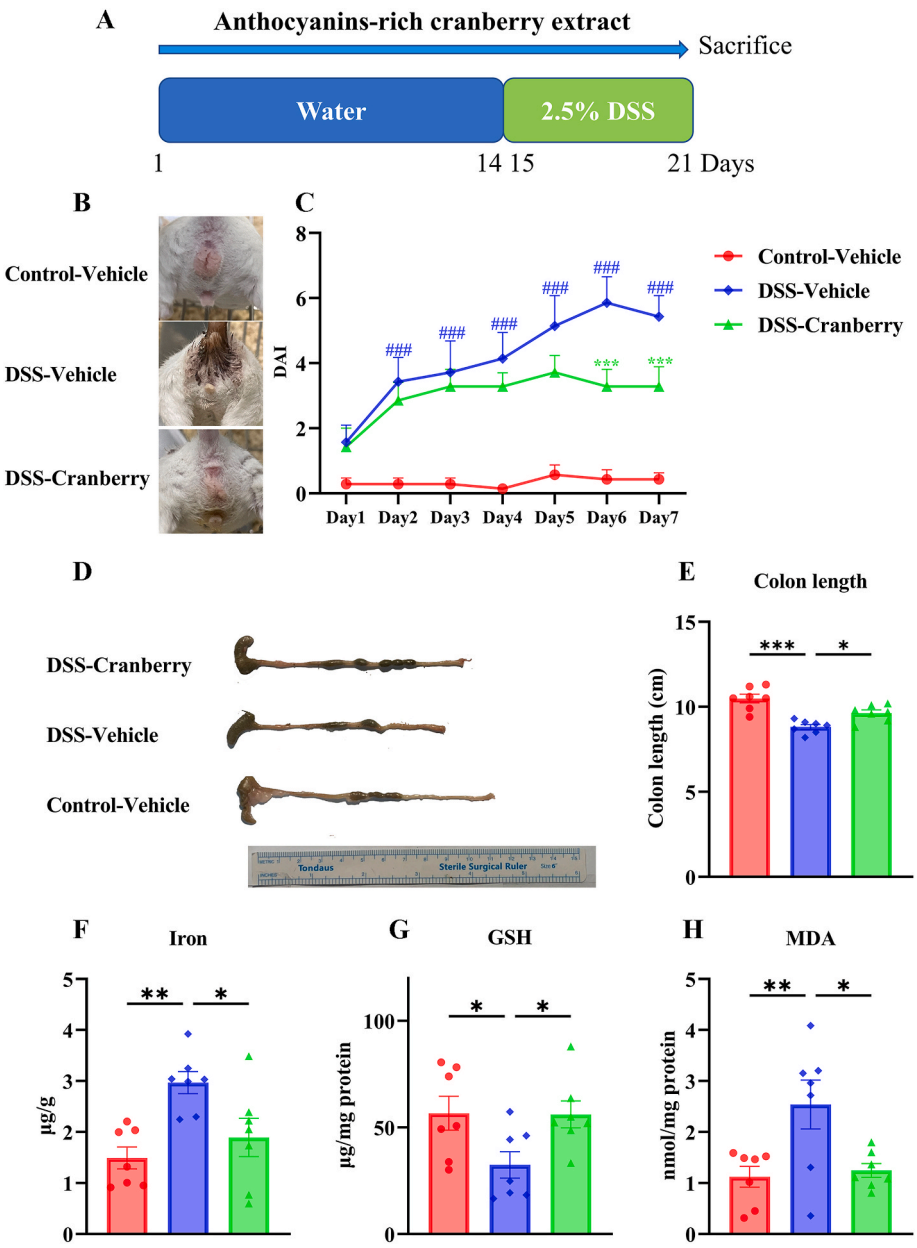

Fig. 2. The therapeutic impact of anthocyanin-rich cranberry extract on DSS-induced IBD in mice. (A) Experimental timeline depicting the administration of water or 2.5% DSS over 21 days with cranberry extract supplementation. (B) Representative images of mice from the Control-Vehicle, DSS-Vehicle, and DSS-Cranberry groups. (C) DAI scores over a 7-day period showing the progression of IBD symptoms and the attenuated effect of cranberry extract (###$p < 0.001$ vs. Control-Vehicle; ***$p < 0.001$ vs. DSS-Vehicle). (D) Comparison of colon morphology and (E) measured colon length among the three groups (*$p < 0.05$, ***$p < 0.001$). (F) Iron concentration, (G) GSH levels, and (H) MDA content in colonic tissue indicating oxidative stress and the antioxidative response induced by cranberry treatment (*$p < 0.05$, **$p < 0.01$). Data are presented as mean ± SEM (n = 7).

extracted ion chromatogram (EIC). Besides, QC samples were analyzed to calculate the relative standard deviation (RSC) of the methods. The EIC isolates and displays the signal for specific ions, providing a clearer resolution of compounds with similar retention times (Supplementary file 2).

2.5. Animals

ICR male mice, 9 weeks old and with an average weight of 26 ± 2 g, were acquired from Slac Animal Center (Shanghai, China). The mice were housed under controlled conditions: temperature at 22 ± 2 °C and humidity at 55 ± 5% after their arrival in animal facility of Huaqiao University. Access to water and standard rodent feed was unrestricted during the study. A 7-day acclimatization period preceded experimental interventions to minimize stress and acclimate the mice to new environmental conditions and handling routines. All procedures adhered to the experimental animal guidelines of Huaqiao University and Chinse government. The study received an ethical approval No. A2022043, dated August 07, 2022 by Experimental Animal Management Committee of Huaqiao University.

2.6. Chemicals and reagents

DSS (D808272, 40000 MW) was purchased from Macklin (Shanghai, China). In efficacy experiment, proinflammatory cytokines kits including interleukin-1 beta (IL-1β) (KE10003), interleukin-6 (IL-6) (KE10091), tumor necrosis factor-alpha (TNF-α) (KE10002) were purchased from Proteintech (Wuhan, China). In FMT experiment,

Table 4
Content of several representative anthocyanins in cranberry extracts.

Chemical Name	CAS No.	Molecular Formula	Content (ng/mg extract)
Cyanidin-3-galactoside	27661-36-5	C21H21ClO11	4963.557
Delphinidin	528-53-0	C15H11ClO7	0.133301
Procyanidin B4	29106-51-2	C30H26O12	296.2992
Cyanidin	528-58-5	C15H11ClO6	118.3818
Procyanidin B2	29106-49-8	C30H26O12	432.7379
Petunidin	1429-30-7	C16H13ClO7	0.540275
Pelargonidin	134-04-3	C15H11ClO5	0.134971
Peonidin	134-01-0	C16H13ClO6	9.800393
Malvidin	643-84-5	C17H15ClO7	0.091552
Rutin	153-18-4	C27H30O16	96.05088
Luteolin	491-70-3	C15H10O6	3.028782
Quercetin	117-39-5	C15H10O7	39.98998
Isorhamnetin	480-19-3	C16H12O7	5.250098
Kaempferol	520-18-3	C15H10O6	1.718566

proinflammatory cytokines kits including IL-1β (ELK1271), IL-6 (ELK1157), TNF-α (ELK1387) were purchased from Elkbiotech (Wuhan, China). Tissue iron (BC4355), malondialdehyde (MDA, BC0025) and glutathione (GSH, BC1175) kits were purchased from Solarbio (Beijing, China). The source of antibody was provided in Table 1.

2.7. Experimental design

Efficacy experiment: Mice were divided into three groups as follows: Control-vehicle, DSS-vehicle, and DSS-cranberry. The DSS-cranberry group consisted of mice that were orally administered with 200 mg/kg cranberry extract once a day. For the preparation of the DSS aqueous solution, DSS was solubilized in sterile water to achieve a concentration of 2.5%. The timeline was provided in Fig. 2A.

Antibiotic intervention experiment: the mice were subjected to random allocation into five distinct groups. These groups were designated as follows: Control-vehicle, DSS-vehicle, DSS-cranberry, DSS-antibiotic, and DSS-cranberry + antibiotic. A specifically formulated antibiotic cocktail was used, comprising a combination of four different antibiotics. The components of this cocktail were ampicillin, metronidazole, neomycin, and vancomycin, each dosage of 9 mg/kg, 9 mg/kg, 9 mg/kg, and 4.5 mg/kg, respectively. Before the cranberry administration, the mice were subjected to a pre-treatment regimen with this antibiotic cocktail. This pretreatment involved administering the cocktail to the mice twice daily from 2 weeks before cranberry administration to the end of the experiment. The timeline was provided in Fig. 8A.

FMT experiment: the procedure was described in the previous study with some modifications (Yang et al., 2023). Briefly, recipient mice were divided into three groups: Control vehicle-FMT, DSS vehicle-FMT, and DSS cranberry-FMT. These recipient mice were firstly injected with ampicillin, metronidazole, neomycin, and vancomycin, each dosage of 9 mg/kg, 9 mg/kg, 9 mg/kg, and 4.5 mg/kg, respectively for 2 weeks before FMT. Donor mice were divided into three groups: Control vehicle, DSS vehicle, and DSS cranberry. Fresh fecal samples from donor mice were collected every day, homogenized in PBS. Recipient mice was orally administrated with the fecal suspension (100 mg/mL) throughout the entire experiment. Administration involved treating these mice with 200 μL of the fecal microbiota solution per day. The timeline was provided in Fig. 9A.

2.8. Evaluation of disease activity index (DAI)

During the whole study, daily monitoring of each mouse was implemented to assess their health and response to treatment. The DAI for each mouse was evaluated on a daily basis. This evaluation was based on a comprehensive tripartite criterion, encompassing key indicators such as weight loss, stool consistency, and the presence of blood in the stool. Each of these indicators was assigned a specific scoring metric, detailed in Table 2, allowing for a quantitative assessment of the disease severity.

2.9. Histopathological evaluation

Colonic tissues collected from the mice were fixed in 4%

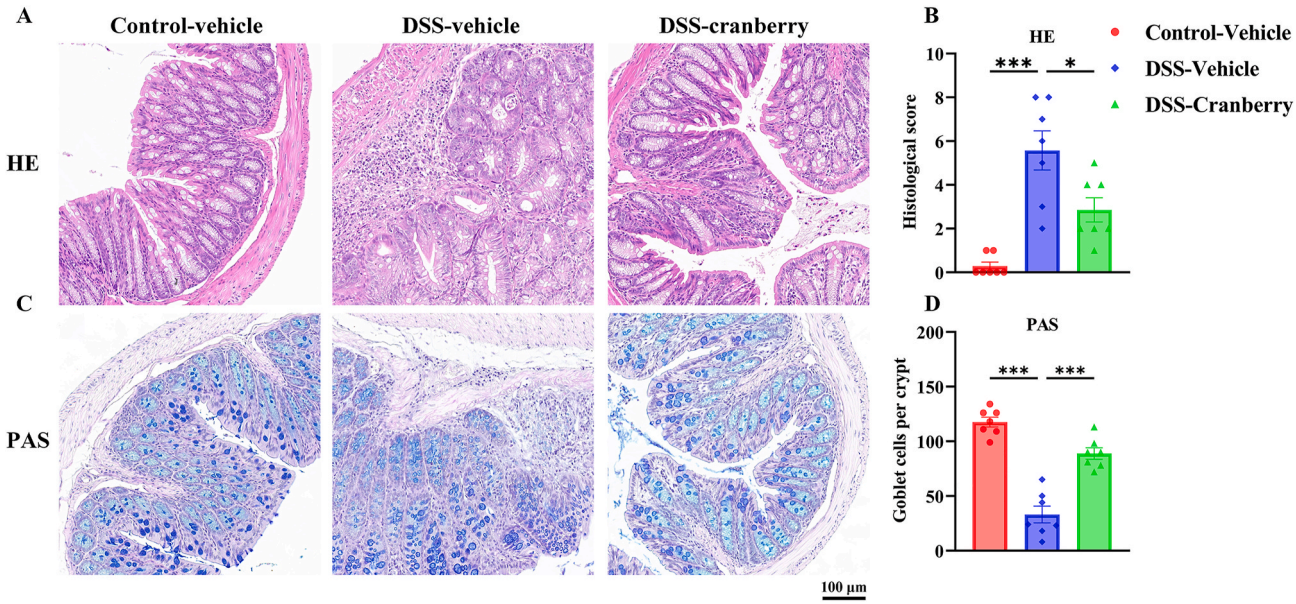

Fig. 3. Histopathological analysis of colonic tissue from IBD-induced mice treated with cranberry extract. (A) HE staining of colon sections from Control-Vehicle, DSS-Vehicle, and DSS-Cranberry groups, showing the structural integrity and inflammatory cell infiltration. (B) Histological scores quantifying the degree of tissue damage and inflammation, with cranberry treatment significantly reducing histological severity in DSS-induced IBD mice (***$p < 0.001$, *$p < 0.05$ compared to DSS-Vehicle). (C) PAS staining indicating goblet cell abundance in the colonic epithelium. (D) Goblet cell counts per crypt, with cranberry treatment maintaining goblet cell numbers despite DSS-induced damage (***$p < 0.001$ compared to DSS-Vehicle). Scale bar = 100 μm. Data represent mean ± SEM (n = 7).

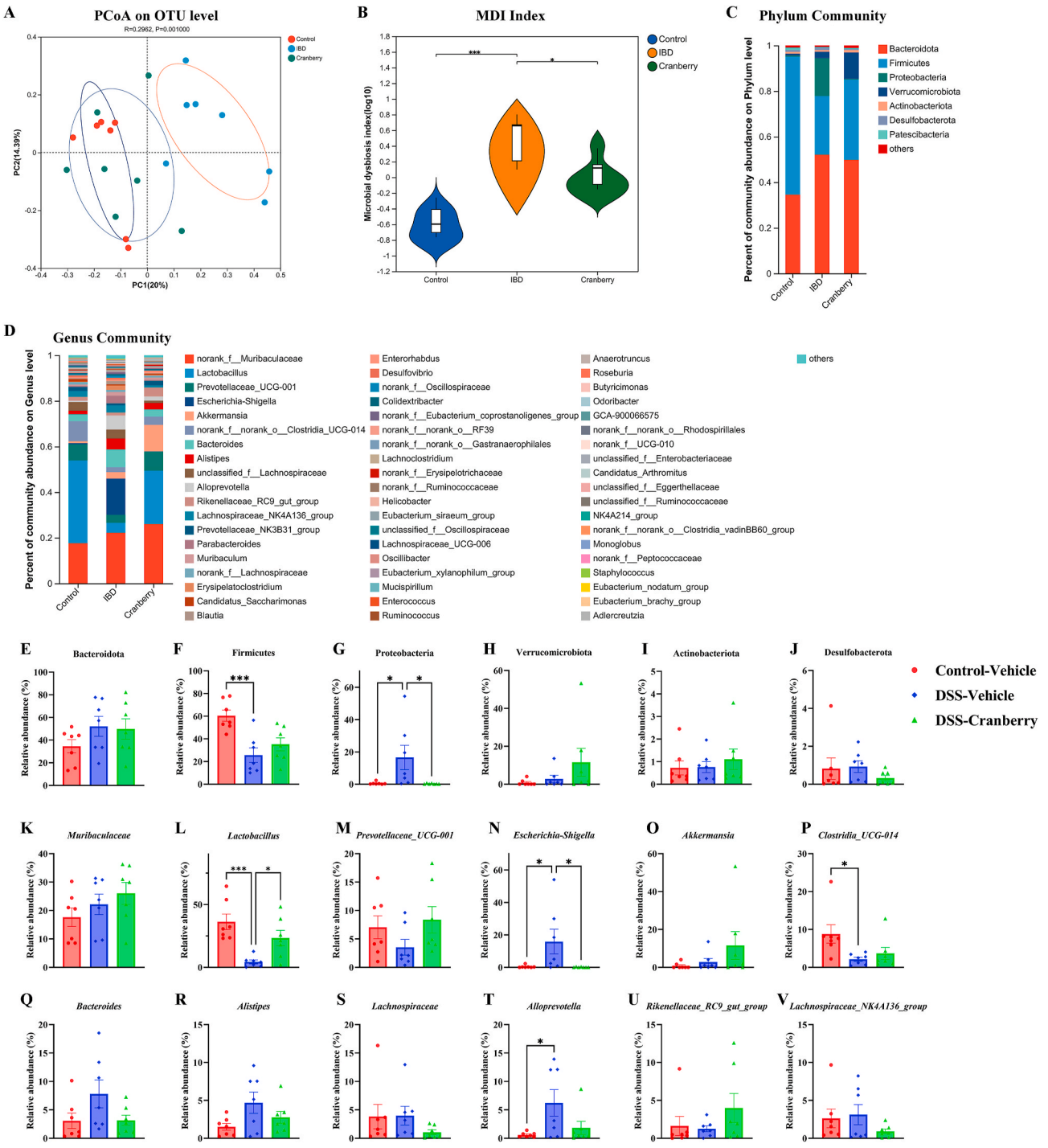

Fig. 4. Microbial diversity and composition analysis in control and IBD-induced mice with and without cranberry extract treatment. (A) Principal coordinate analysis (PCoA) on OTU level showing distinct clustering of microbial communities among Control, IBD, and Cranberry-treated groups, with significant separation (PERMANOVA $p < 0.001$). (B) MDI revealing increased diversity in Cranberry-treated compared to IBD mice (***$p < 0.001$). (C) Phylum-level distribution of microbial communities highlighting shifts in bacterial populations. (D) Genus-level community composition depicted in stacked bar charts, with notable changes in key bacterial genera among groups. Relative abundance of bacterial phyla: (E) Bacteroidetes, (F) Firmicutes, (G) Proteobacteria, (H) Verrucomicrobia, and (I) Actinobacteria, and (J) Desulfobacterota, indicating significant variations. (K–U) Relative abundance of specific bacterial genera and groups, demonstrating alterations in the gut microbiome due to IBD and its modulation by cranberry treatment. Data are presented as mean ± SEM (n = 7); *$p < 0.05$, **$p < 0.01$, ***$p < 0.001$ indicate statistical significance across the groups.

paraformaldehyde for 24 h. Subsequently, they were embedded in paraffin wax for histopathological analysis. Paraffin blocks were sectioned at a thickness of 5 μm using a microtome. These sections were then subjected to deparaffinization in xylene and rehydrated through a graded series of ethanol solutions, culminating in distilled water. For Hematoxylin and Eosin (H&E) staining, the sections were stained with Harris hematoxylin for a duration of 5 min, followed by a brief differentiation in 1% acid alcohol. A blueing step was performed in 0.2% ammonia water for a maximum of 1 min, and counterstaining was achieved with eosin for 2 min. In the case of Periodic Acid-Schiff (PAS)

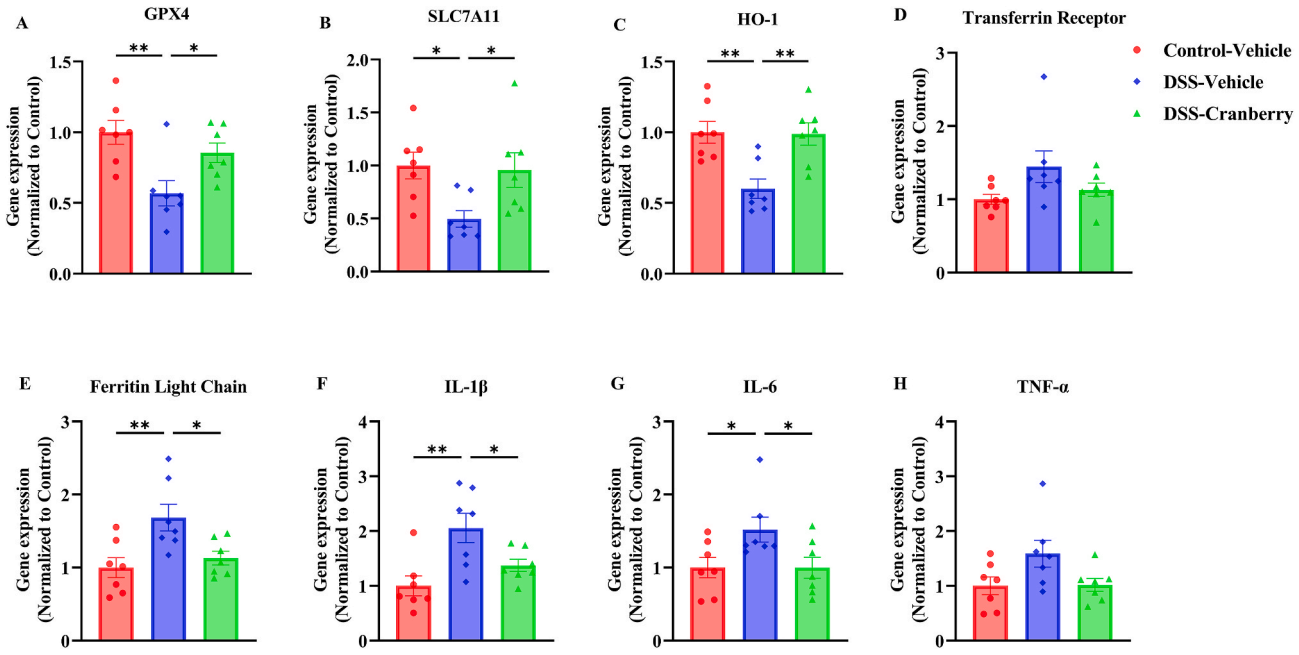

Fig. 5. Gene expression analysis in colonic tissue of IBD-induced mice treated with cranberry extract. (A–H) Relative expression levels of genes associated with ferroptosis and inflammation in Control-Vehicle, DSS-Vehicle, and DSS-Cranberry groups. (A) GPX4, (B) SLC7A11, (C) HO-1, and (E) ferritin light chain gene expressions were not significantly altered by cranberry treatment. (D) Transferrin receptor levels indicate no change. (F) IL-1β and (G) IL-6 show a significant decrease, whereas (H) TNF-α expression is not inhibited in the DSS-Cranberry group compared to DSS-Vehicle. Data presented as mean ± SEM (n = 7); *p < 0.05, **p < 0.01 indicate statistical significance.

staining, the sections were oxidized in 0.5% periodic acid for 10 min, then immersed in Schiff's reagent for 15 min. A subsequent water rinse was employed to develop the characteristic magenta coloration. Both H&E and PAS stained sections were dehydrated through a series of alcohol immersions, cleared in xylene, and mounted with a resinous medium. The prepared slides were then examined under a light microscope according to the detailed criterion including morphological and structural aspects in Table 3.

2.10. Biochemical analysis

Colonic tissues, carefully dissected from the animals, were homogenized according to the commercial kits. This homogenization was performed in a specialized buffer solution, the composition of which was provided by the respective commercial kits intended for subsequent biochemical analyses. The contents of iron, MDA and GSH in colon homogenates, were quantitatively assessed. The levels of IL-1β, IL-6 and TNF-α in colonic tissues were measured by ELISA kits. Throughout the process, strict adherence to the manufacturer's instructions was maintained to ensure accuracy and reliability of the results.

2.11. qRT-PCR

Colonic tissues were collected from the mice after length measurement, initiating the process of total RNA extraction. The tissues were first homogenized, and then treated with reagents that facilitated the isolation of RNA. After isolation, the RNA was reverse transcripted to cDNA. The real-time PCR reaction was performed using a thermal cycler. This process unfolded in distinct cycles, each comprising stages of denaturation (at 95 °C for 30 s), annealing (at 53 °C for 60 s), and extension (at 72 °C for 60 s). For quantitative analysis, the expression of targeted genes including GPX4 (with forward primer TGTGGAAGTGGCTGAAGGAG and reverse primer CCCTCACGGTTGATAAGAAA), SLC7A11 (with forward primer TGCTTTGGGTCTATGAATGG and reverse primer TGCTTTGGGTCTATGAATGG), HO-1 (with forward primer AGGTACACATCCAAGCCGAGA and reverse primer CATCACCAGCTTAAAGCCTTCT), transferrin receptor (with forward primer TCACACTCTCTCAGCTTTAGTG and reverse primer TGGTTTCTGAAGAGGGTTTCAT), ferritin light chain (with forward primer TGGCCATGGAGAAGAACCTGAATC and reverse primer GGCTTTCCAGGAAGTCACAGAGAT), IL-1β (with forward primer 5′-TGCCACCTTTTGACAGTGATG-3′ and reverse primer 5′-TGATGTGCTGCTGCGAGATT-3′), IL-6 (with forward primer 5′-CCCCAATTTCCAATGCTCC-3′ and reverse primer 5′-CGCACTAGGTTTGCCGAGTA-3′), TNF-α (with forward primer 5′-GATCGGTCCCCAAAGGGATG-3′ and reverse primer 5′-CCACTTGGTGGTTTGTGAGTG-3′) were measured. The expression was then normalized to the expression of internal gene GAPDH (with forward primer TGAGGCCGGTGCTGAGTATGT and reverse primer CAGTCTTCTGGGTGGCAGTGAT). The $2^{-\Delta\Delta CT}$ method, which leverages the Ct values, was applied to calculate the relative expression of the targeted genes by normalization with GAPDH.

2.12. Immunofluorescence

Colonic tissues were collected after length measurement and promptly rinsed in PBS, followed by fixation in 4% paraformaldehyde at 4 °C for 24 h. After fixation, tissues were dehydrated in sucrose solution and then embedded in OCT. The tissues containing OCT was subjected to freezing in liquid nitrogen rapidly. These preparations were then stored at −80 °C until required for sectioning. For the production of tissue sections, a cryostat, maintained at approximately −27 °C, was utilized to slice the tissues into 15 μm thick sections. These sections were carefully mounted on slides coated with poly-L-lysine to enhance adhesion and subsequently stored at −20 °C. Prior to immunostaining, a brief refixation in 4% paraformaldehyde was performed, followed by a thorough rinse in TBS containing Triton X-100. The sections were then incubated in a blocking solution composed of 5% goat serum and 0.3% Triton X-100 in TBS for 1 h. For the detection of targeted proteins, sections were incubated overnight with primary antibodies, all at dilutions (Table 1) recommended by the manufacturer. This incubation occurred in a friger at 4 °C. Following primary antibody incubation,

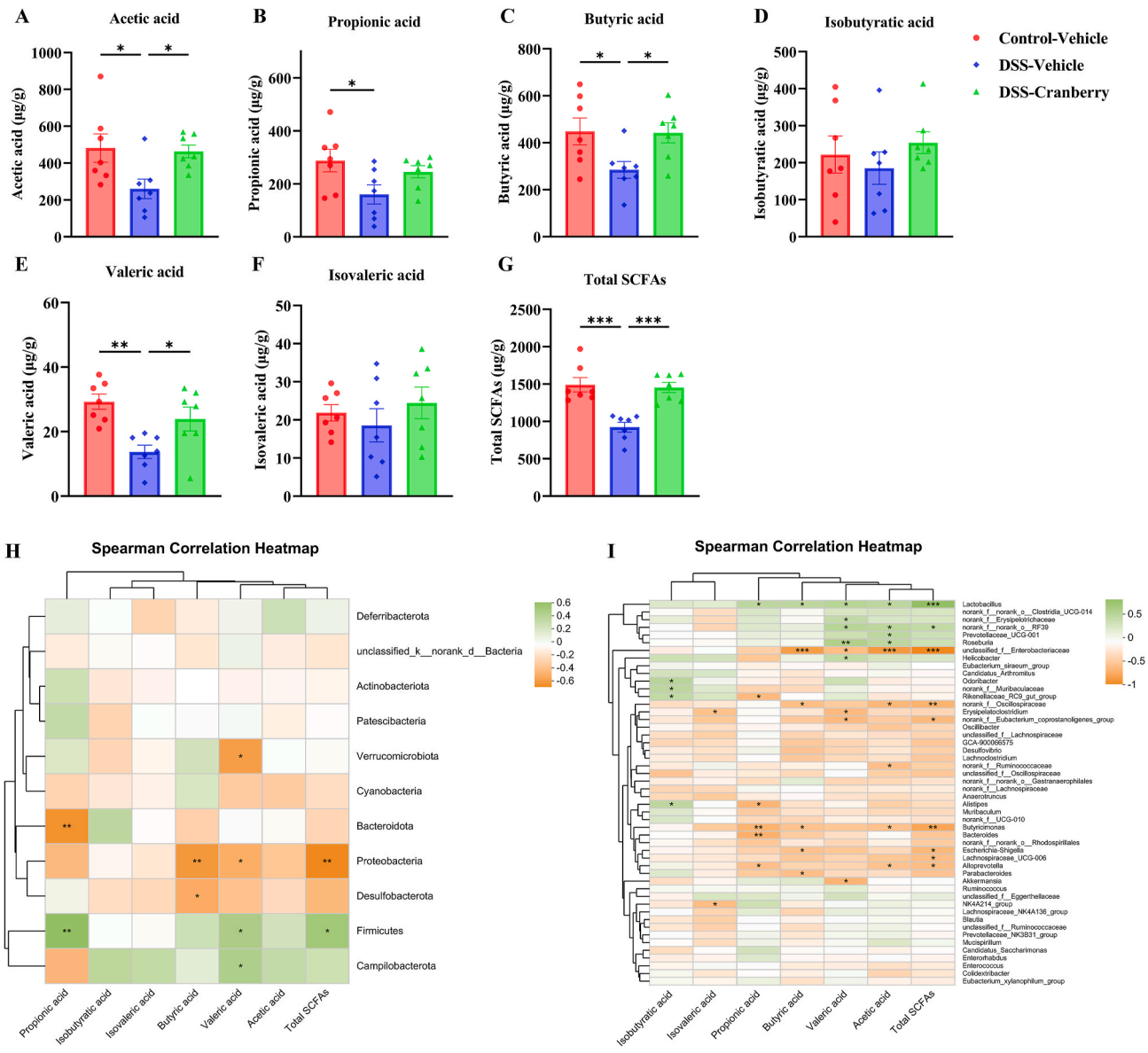

Fig. 6. SCFAs profiles and microbial correlations in IBD-induced mice treated with cranberry extract. Concentrations of various SCFAs in colonic contents: (A) Acetic acid, (B) Propionic acid, (C) Butyric acid, (D) Isobutyric acid, (E) Valeric acid, and (F) Isovaleric acid, with cranberry extract increasing the levels of butyric acid and total SCFAs (G) in comparison to the control and DSS-vehicle groups. Spearman correlation heatmaps showing the association between SCFAs and gut microbiota composition at the phylum level (H) and at a more detailed taxonomic resolution (I), with significant correlations highlighted (*p < 0.05, **p < 0.01, ***p < 0.001). Data are represented as mean ± SEM (n = 7).

fluorophore-conjugated secondary antibodies were applied to the sections and incubated for 3 h under dim lighting conditions. To stain cell nuclei, a DAPI-containing antifade medium was applied. The stained sections were then examined and photographed under a Leica TCS SP8 confocal microscope. Imaris was used to analyze the images.

2.13. SCFAs measurement

The concentration of SCFAs in the fecal was quantified using gas chromatography. For the collection of samples, fresh feces from mice, weighing approximately 200 mg, were gathered. These fecal samples were then homogenized in 1 mL of deionized water. Following homogenization, the mixture was place to centrifuge at 12,000×*g* for 10 min. Subsequently, 1 mL of this supernatant was carefully extracted and mixed with 100 μL of concentrated hydrochloric acid. To this acidified supernatant, 5 mL of ether was added, thoroughly mixed, and allowed to stand for extraction at room temperature for 20 min. After extraction, the organic phase was further clarified by centrifugation at 3500×*g* for 10 min. The resulting clear supernatant was then utilized for SCFA analysis.

2.14. 16 S rRNA gene sequencing

The extraction of DNA from fecal samples utilized a dedicated stool DNA extraction kit. For amplifying the V3 and V4 hypervariant regions of the bacterial 16 S rRNA gene, specific primer sets were used: forward primer 338 F (5′-ACTCCTACGGGAGGCAGCAG-3′) and reverse primer 806 R (5′-GGACTACHVGGGTWTCTAAT-3′). Post-PCR amplification, the amplified products underwent 2% agarose gel electrophoresis for identification of the targeted DNA segments. The relevant DNA fragments were then recovered from the agarose gel through the AMPure XT beads kit. Sequencing of these fragments was performed on the MiSeq System, employing a paired-end sequencing method that produced reads of 2 × 300 bp. Operational Taxonomic Units (OTUs) were formed by clustering

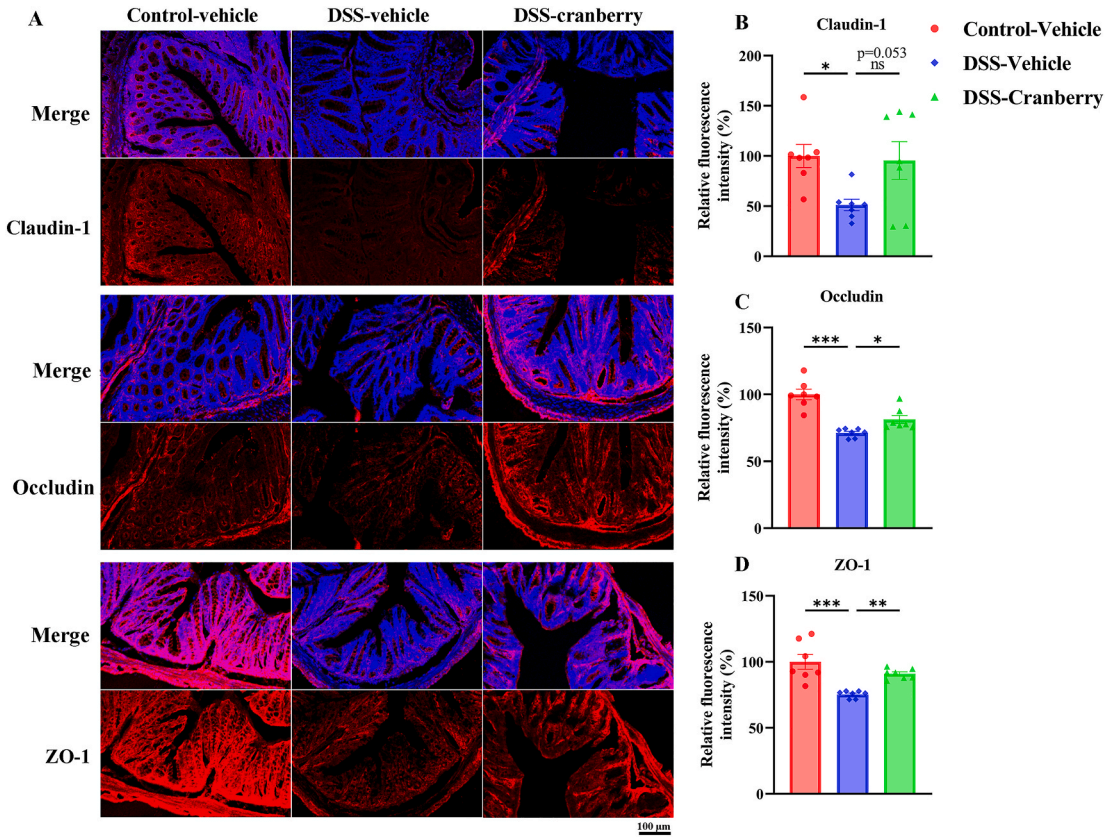

Fig. 7. Cranberry induced tight junction protein levels in colon. (A) Representative images depicting the expression of claudin-1, occludin, and ZO-1 in the Control-Vehicle, DSS-Vehicle, and DSS-Cranberry groups. Quantitative analysis of fluorescence intensity is shown for (B) claudin-1, (C) occludin, and (D) ZO-1. Cranberry increased the levels of claudin-1 ($p = 0.053$), occludin, ZO-1 compared to DSS-Vehicle group. Data points represent individual mice, with bar heights indicating the mean ± SEM ($n = 7$); *$p < 0.05$, **$p < 0.01$, ***$p < 0.001$ indicate statistical differences between groups.

the sequences based on a 97% similarity threshold, a widely accepted standard for bacterial species differentiation. Beta diversity indices were calculated to quantitatively assess the bacterial community diversity within each sample. Additionally, beta diversity analysis was implemented to compare microbial compositions among various samples, providing insight into microbial ecosystem variations across different groups. Principal Coordinates Analysis (PCoA) was used to graphically represent and interpret the bacterial community structure differences, utilizing weighted UniFrac distances for dimensionality reduction, thereby simplifying complex microbial community data. Hierarchical clustering analysis was also performed, graphically displaying the similarities and divergences in microbial community structures among the samples.

2.15. Statistical analysis

Data are expressed as mean ± SEM. For the purpose of evaluating differences between groups, a one-way ANOVA followed by a further Tukey's post hoc test was performed. In the interpretation of these statistical results, a p-value threshold of less than 0.05 was established as the criterion for statistical significance.

3. Results

3.1. The content of anthocyanins after extraction and purification

Firstly, the anthocyanin content of cranberry juice was 762.38 μg/g cranberry, while the anthocyanin content of crude extract was 702.73 μg/g cranberry, indicating that 92.18 % of anthocyanins was extracted. After purification with AB-8 resin, the anthocyanin content of anthocyanins-rich cranberry extract was 302.62 mg/g lyophilized powder.

3.2. Quantification of anthocyanins in cranberry extract by UPLC

In the subsequent phase of our analysis, UPLC spectroscopy was utilized to conduct a quantification of the anthocyanin within the anthocyanins-rich cranberry extract. Fourteen representative anthocyanins were selected and the standard curves were established. As shown in Fig. 1 and Table 4, the extract contains 4963 ng/mg cyanidin-3-galactoside, 432 ng/mg procyanidin B2, 296 ng/mg procyanidin B4, 118 ng/mg cyanidin. The content of delphinidin, petunidin, pelargonidin and malvidin was relatively low in the cranberry extract.

3.3. Anthocyanins-rich cranberry extract supplementation attenuated DSS-induced IBD symptoms in mice

As shown in Fig. 2, anthocyanins-rich cranberry extract significantly reduced symptoms of DSS-induced IBD in mice. Notably, symptoms like diarrhea, indicative of colonic inflammation, were notably alleviated (Fig. 2B). A marked decrease in the DAI was observed in cranberry extract-treated mice, indicating reduced severity of IBD symptoms (Fig. 2C). Additionally, an increase in colon length in cranberry-treated mice suggested reduced colonic damage (Fig. 2D and E). On the other hand, the biochemical measurement found that colonic iron and MDA contents were significantly induced by DSS, however, cranberry reversed the elevation. Similarly, cranberry also reversed the reduction of GSH content in colonic tissues (Fig. 2F–H).

HE staining revealed that normal mice displayed no significant pathological changes, maintaining healthy colonic mucosa. In contrast,

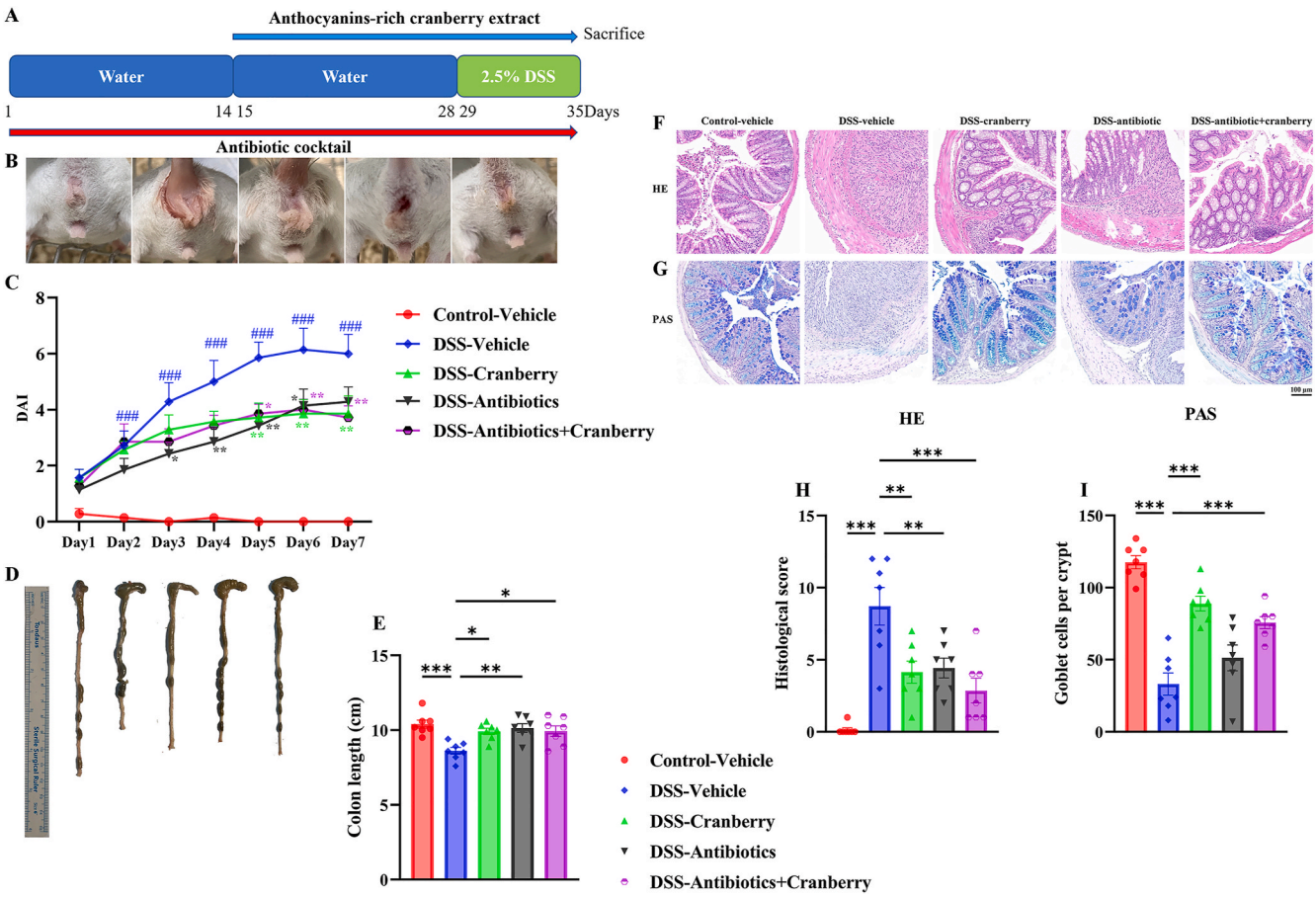

Fig. 8. Evaluation of the efficacy of cranberry with antibiotic pretreatment in DSS-induced IBD mice. (A) Schematic timeline showing the experimental design, including periods of water, DSS, antibiotic cocktail, and anthocyanins-rich cranberry extract administration until sacrifice. (B) Representative images of mice from each group depicting the progression of symptoms. (C) DAI over a 7-day period for Control-Vehicle, DSS-Vehicle, DSS-Cranberry, DSS-Antibiotics, and DSS-Antibiotics + Cranberry groups, indicating the effect of treatments on IBD symptoms (###$p < 0.001$ vs. Control-Vehicle; *$p < 0.05$, **$p < 0.01$, ***$p < 0.001$ vs. DSS-Vehicle). (D) Visual comparison of colon morphology and (E) quantification of colon length, showing cranberry extract's influence on colon size (*$p < 0.05$, **$p < 0.01$, ***$p < 0.001$). (F) HE and (G) PAS staining of colon sections for histopathological assessment. (H) Histological scores and (I) goblet cell counts per crypt demonstrate the protective role of cranberry against tissue damage and its effect on mucosal health, even after antibiotic pretreatment (***$p < 0.001$, **$p < 0.01$). Scale bar = 100 μm. Data represent mean ± SEM (n = 7).

DSS-induced IBD mice showed distorted glandular architecture, crypt abscesses, and ulceration. Treatment with cranberry extract resulted in a partial preservation of colonic architecture and reduced neutrophilic infiltration, indicating a reduction in inflammation (Fig. 3A and B). PAS staining demonstrated a higher mucin content and increased number of goblet cells in cranberry extract-treated mice compared to the DSS-induced group, suggesting a protective effect on colonic tissues (Fig. 3C and D).

3.4. Reshape of intestinal flora by anthocyanins-rich cranberry extract in IBD mice

β-Diversity, a measure used to assess variations across microbial communities, was evaluated through principal coordinate analysis (PCoA). This analysis successfully differentiated the control group from the DSS-treated group, indicating significant microbial community variation. Interestingly, the microbial community of anthocyanins-rich cranberry extract group exhibited similarities to that of the control group, suggesting a therapeutical effect of cranberry on DSS-induced alterations (Fig. 4A). Furthermore, the microbial dysbiosis index (MDI), formulated specifically for this study population via a compositional data analysis approach that corrects for compositionality through renormalization and permutation (Gunathilake et al., 2020), showed an increase in MDI following DSS treatment. In contrast, cranberry supplementation markedly reduced the MDI, indicating its potential to restore microbial balance in IBD-affected mice (Fig. 4B). Further comparative analyses of the gut microbiota composition at both phylum and genus levels highlighted distinct differences across the groups (Fig. 4C and D). Bacteroidota and Firmicutes emerged as the predominant phyla, with *Muribaculaceae* and *Lactobacillus* ranking as the most abundant genera in the gut flora of mice. Analysis of the top six phylum revealed that DSS treatment significantly altered the microbial balance by reducing the relative abundance of Firmicutes and increasing the relative abundance of Proteobacteria. However, cranberry supplementation effectively counteracted the DSS-induced shift in Proteobacteria levels (Fig. 4G). Among the top twelve phyla, notable changes were observed where DSS treatment led to a decrease in *Lactobacillus* and *Clostridia_UCG-014* and an increase in *Escherichia-Shigella*. Conversely, cranberry supplementation was associated with an increased relative abundance of *Lactobacillus* and a decreased presence of *Escherichia--Shigella*, exhibiting its beneficial impact on the gut microbiota composition (Fig. 4L–N).

3.5. Attenuation of ferroptosis and inflammation associated gene expression in IBD mice by anthocyanins-rich cranberry extract

The influence of anthocyanins-rich cranberry extract supplementation on ferroptosis and inflammation was assessed through the

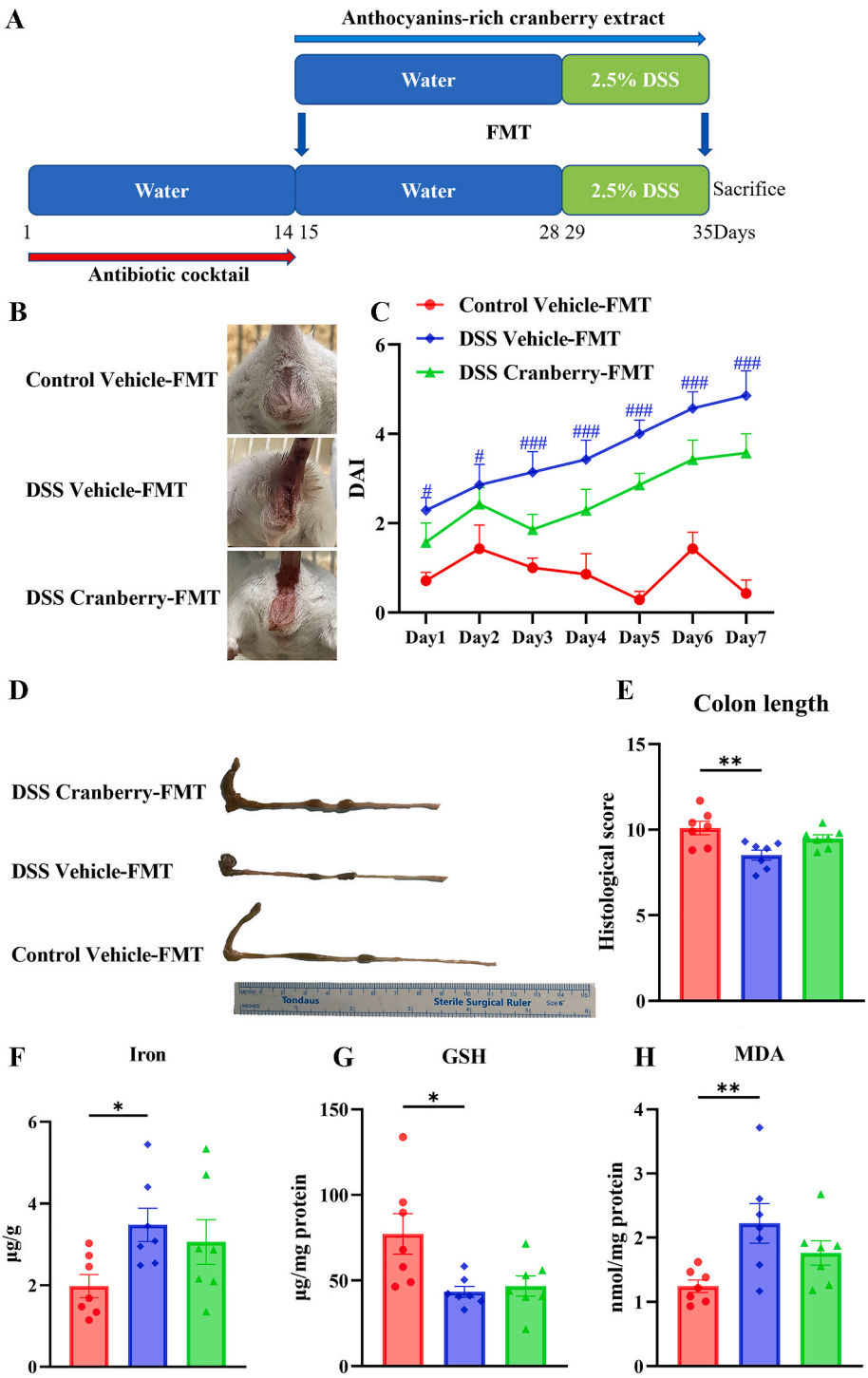

Fig. 9. Anthocyanin-rich cranberry extract FMT did not cause any alteration on DSS-induced IBD in mice. (A) Experimental timeline depicting the administration of water or 2.5% DSS over 21 days with cranberry FMT. (B) Representative images of mice from the Control Vehicle-FMT, DSS Vehicle-FMT, and DSS Cranberry-FMT groups. (C) DAI scores over a 7-day period showing the progression of IBD symptoms (#$p < 0.05$ and ###$p < 0.001$ vs. Control Vehicle-FMT). (D) Comparison of colon morphology and (E) measured colon length among the three groups (**$p < 0.01$). (F) Iron concentration, (G) GSH levels, and (H) MDA content in colonic tissue (*$p < 0.05$, **$p < 0.01$). Data are presented as mean ± SEM (n = 7).

evaluation of associated gene expression within colonic tissues. As illustrated in Fig. 5, expressions of GPX4, SLC7A11, and HO-1 were found to be significantly reduced in the DSS-treated group. In contrast, these expressions were significantly elevated following treatment with cranberry. Furthermore, the increase in ferritin light chain expression induced by DSS was effectively attenuated with cranberry supplementation. Additionally, elevated expressions of cytokines, including IL-1β, IL-6, and TNF-α, which were observed in the DSS group, were suppressed by the administration of cranberry, indicating a potential ameliorative effect on the abnormal cytokine expression triggered by DSS.

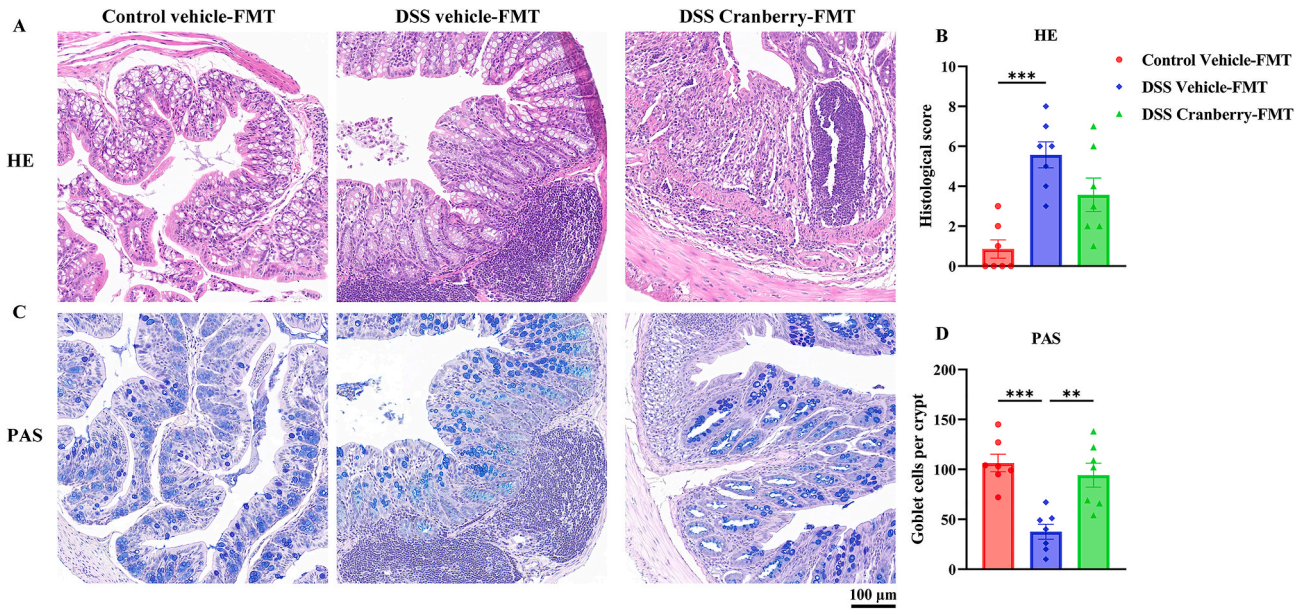

Fig. 10. Histopathological evaluation of colonic tissues following FMT with cranberry. (A) HE staining displays the colonic architecture across Control Vehicle-FMT, DSS Vehicle-FMT, and DSS Cranberry-FMT groups, indicating inflammation and structural integrity. (B) Histological scoring quantifies tissue damage, with cranberry-FMT did not decrease histological severity compared to DSS Vehicle-FMT. (C) PAS staining highlights goblet cell density within the colonic epithelium. (D) Goblet cell counts per crypt demonstrate no alteration between cranberry-FMT and vehicle-FMT groups. Scale bar = 100 μm. Data are expressed as mean ± SEM (n = 7) with statistical significance denoted as $^{**}p < 0.01$, $^{***}p < 0.001$ compared to the DSS Vehicle-FMT group.

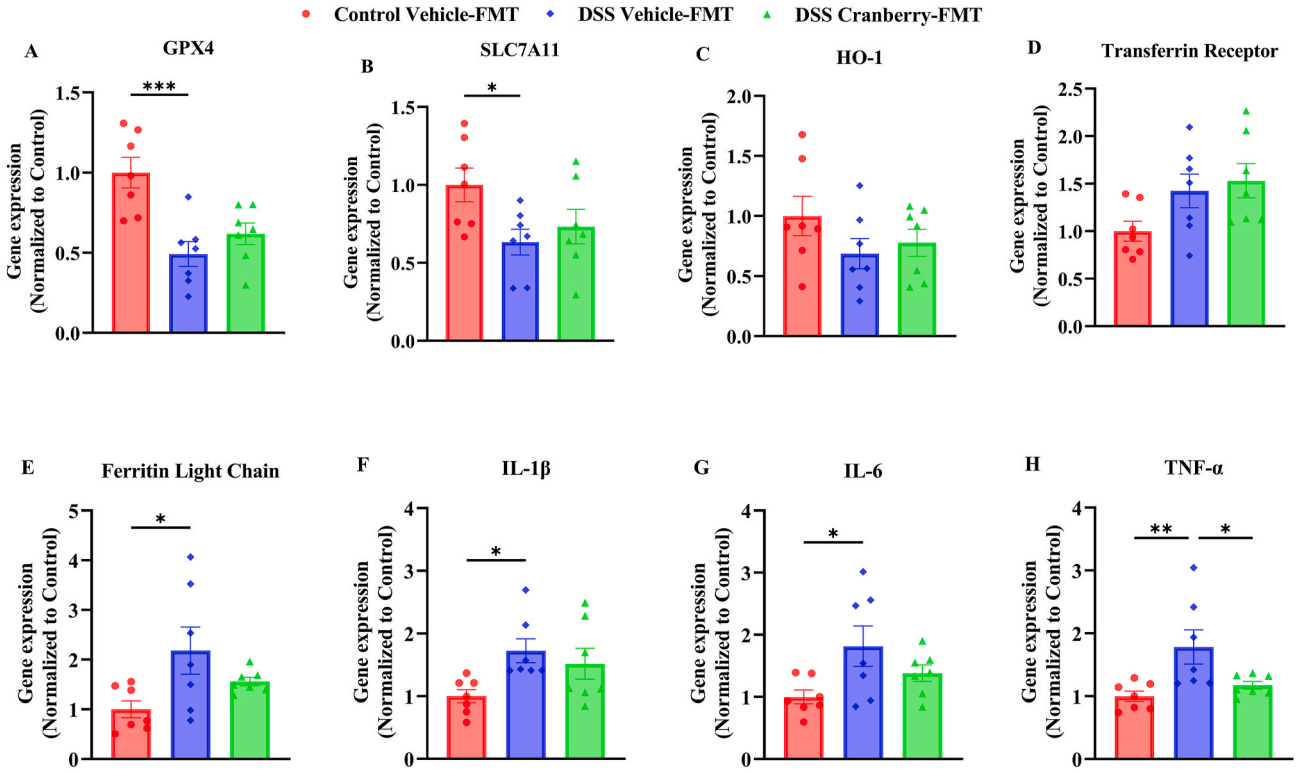

Fig. 11. Gene expression analysis of ferroptosis and inflammation-related markers in FMT-treated mice. (A–H) Bar graphs representing relative gene expression levels in colonic tissues from Control Vehicle-FMT, DSS Vehicle-FMT, and DSS Cranberry-FMT groups: (A) GPX4, (B) SLC7A11, (C) HO-1, (D) Transferrin Receptor, (E) Ferritin Light Chain, (F) IL-1β, (G) IL-6, and (H) TNF-α. Cranberry-FMT did not significantly alter the expression of ferroptosis-related genes except for a decrease in TNF-α. Data are normalized to control and presented as mean ± SEM (n = 7); $^{*}p < 0.05$, $^{**}p < 0.01$, $^{***}p < 0.001$ indicate statistical significance compared to the DSS-vehicle group.

3.6. *Upregulation of SCFAs by anthocyanins-rich cranberry extract*

Subsequent analyses were focused on measuring SCFAs, including acetic acid, propionic acid, butyric acid, isobutyratic acid, valeric acid, and isovaleric acid, in the fecal samples (Fig. 6). The results showed a notable decrease in the levels of acetic acid, propionic acid, butyric acid

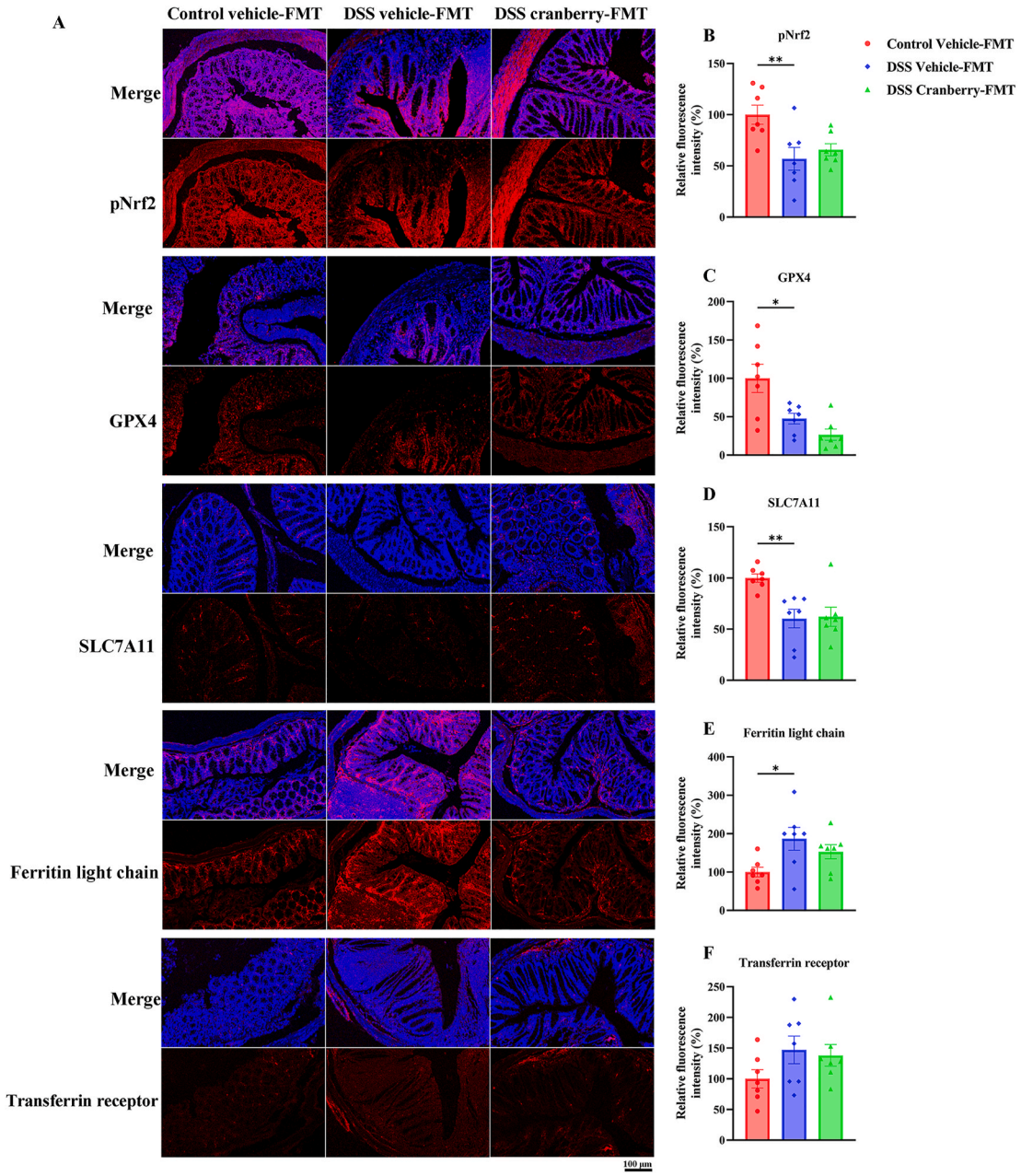

Fig. 12. Immunofluorescence analysis of ferroptosis-related proteins in colonic tissues following FMT treatment. (A) Representative images depicting the expression of pNrf2, GPX4, SLC7A11, ferritin light chain, and transferrin receptor in the Control Vehicle-FMT, DSS Vehicle-FMT, and DSS Cranberry-FMT groups. The images show the localization and intensity of protein expression, with red indicating the specific protein and blue representing the cell nuclei. Quantitative analysis of fluorescence intensity is shown for (B) pNrf2, (C) GPX4, (D) SLC7A11, (E) ferritin light chain, and (F) transferrin receptor, demonstrating a non-significant alteration in these ferroptosis associated proteins in the DSS Cranberry-FMT group compared to DSS Vehicle-FMT. Data are normalized to control values and presented as mean ± SEM (n = 7); *p < 0.05, **p < 0.01 indicate statistical significance. Scale bar = 100 μm. (For interpretation of the references to color in this figure legend, the reader is referred to the Web version of this article.)

and valeric acid in IBD mice. However, this decline of acetic acid, butyric acid and valeric acid was reversed following supplementation with anthocyanins-rich cranberry extract. Furthermore, cranberry extract was found to increase the total SCFA content, which had been reduced in the fecal of IBD mice by DSS. Besides, by using Spearman correlation heatmap analysis, we found that, at the phylum level, Firmicutes was positively correlated with propionic acid, valeric acid and total SCFAs, while Proteobacteria was negatively correlated with butyric acid, valeric acid and total SCFAs. At the genus level, *Lactobacillus* was positively correlated with acetic acid, propionic acid, butyric acid, valeric acid and total SCFAs, while *Escherichia-Shigella* was negatively correlated with butyric acid and total SCFAs.

3.7. Preservation of the intestinal barrier by anthocyanins-rich cranberry extract

The disruption of the intestinal barrier, marked by a reduction or loss of tight junction proteins, is a critical aspect of IBD, leading to altered distribution and increased permeability of the intestinal mucosa. As shown in Fig. 7, by using immunofluorescence staining with key tight junction proteins (claudin-1, occludin, ZO-1), our findings indicated that DSS consumption led to a significant reduction in the levels of these proteins (tented to be significant for claudin-1), suggesting a compromised intestinal barrier. In contrast, mice supplemented with anthocyanins-rich cranberry exhibited an upregulation in the expression

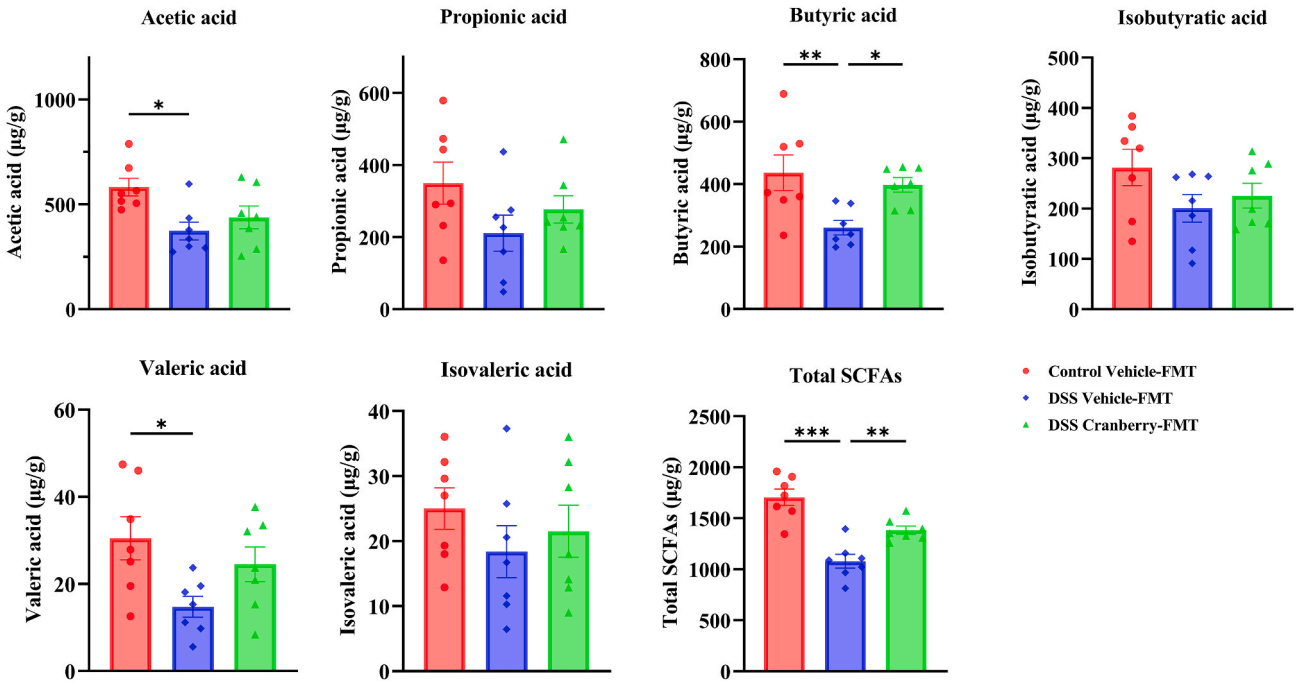

Fig. 13. SCFAs concentrations in fecal samples from FMT-treated mice. The bar graphs illustrate the levels of (A) Acetic acid, (B) Propionic acid, (C) Butyric acid, (D) Isobutyric acid, (E) Valeric acid, (F) Isovaleric acid, and (G) Total SCFAs measured in Control Vehicle-FMT, DSS Vehicle-FMT, and DSS Cranberry-FMT groups. Cranberry-FMT significantly increased the concentrations of butyric acid and total SCFAs compared to DSS Vehicle-FMT, whereas other individual SCFA levels did not show a significant increase. Data points represent individual mice, with bar heights indicating the mean ± SEM (n = 7); *p < 0.05, **p < 0.01, ***p < 0.001 indicate statistical differences between groups.

of these critical proteins, thereby indicating an enhancement of intestinal barrier integrity.

3.8. Antibiotic intervention did not abolish the effects of cranberry extract

To assess the necessity of intestinal flora for the beneficial effects of cranberry on IBD, we initiated gut microbiota depletion through antibiotic pretreatment before administering cranberry (Fig. 8). Initially, we observed that cranberry administration reduced the DAI in DSS-induced IBD mice, and this protective effect persisted even after antibiotic intervention. Furthermore, the study revealed that depleting microbiota with antibiotics did not negate the ability of cranberry to improve colon length. Histological evaluations, including HE and PAS staining, supported these findings; cranberry continued to attenuate histological changes in DSS-induced IBD mice following antibiotic intervention. Specifically, PAS staining showed that cranberry treatment could still restore goblet cell numbers despite the depletion of gut microbiota. Although antibiotic intervention also lessened IBD symptoms and colonic lesions, the inability to fully attribute the therapeutic action of cranberry to intestinal flora modulation alone arises from the complexity of antibiotic interventions. This suggests further investigation is needed to conclusively determine the role of gut microbiota in the efficacy of cranberry against IBD.

3.9. Cranberry FMT did not exert therapeutical efficacy against IBD

To address the limitations observed in the antibiotic intervention experiment and further investigate the influence of cranberry on ferroptosis via a gut microbiota-dependent mechanism, we conducted a FMT experiment. This involved extracting intestinal microbiota from the feces of cranberry-treated mice and transplanting it into recipient mice daily, as shown in Fig. 9. Upon assessing clinical symptoms and pathological damage in mice, we observed no notable improvements in these parameters in IBD mice, including measures of the DAI and colon length. Moreover, the antioxidant capacity of colon tissue remained unchanged post-cranberry-FMT treatment, with levels of iron, MDA, and GSH similar to those observed in DSS-induced IBD mice.

Additionally, the FMT did not ameliorate DSS-induced lesions, such as colon tissue damage and depletion of goblet cells, as shown in Fig. 10, after the transplantation of gut microbiota from cranberry-treated mice. These findings lead to the conclusion that the beneficial effects of cranberry on IBD do not necessitate the involvement of the intestinal flora.

3.10. Cranberry FMT did not regulate ferroptosis and inflammation associated gene expression

Subsequently, we investigated if FMT could influence ferroptosis and inflammation in intestinal inflammation, inspired by previous research indicating FMT from phlorizin alleviated DSS-induced IBD through ferroptosis inhibition (Cheng et al., 2023). qRT-PCR analysis demonstrated that the expression of ferroptosis-related genes, such as GPX4, SLC7A11, HO-1, transferrin receptor, and ferritin light chain, remained unchanged following cranberry FMT. Regarding inflammation-related genes, cranberry FMT only reduced TNF-α levels, with no significant impact on IL-1β and IL-6 (Fig. 11). Additionally, immunofluorescence analysis confirmed that cranberry FMT did not alter the relative fluorescence intensity of proteins including pNrf2, GPX4, SLC7A11, transferrin receptor, and ferritin light chain, as shown in Fig. 12. Collectively, these findings suggest that the positive effects of cranberry treatment on ferroptosis and inflammation in IBD are not effectively conveyed through FMT.

3.11. Cranberry FMT partly increased the content of SCFAs in fecal of IBD mice

Following the cranberry FMT, the levels of SCFAs were also measured. Fig. 13 illustrates that, in comparison to mice receiving vehicle-FMT, the cranberry-FMT group experienced a significant rise in butyric acid and overall SCFA content. However, when comparing the

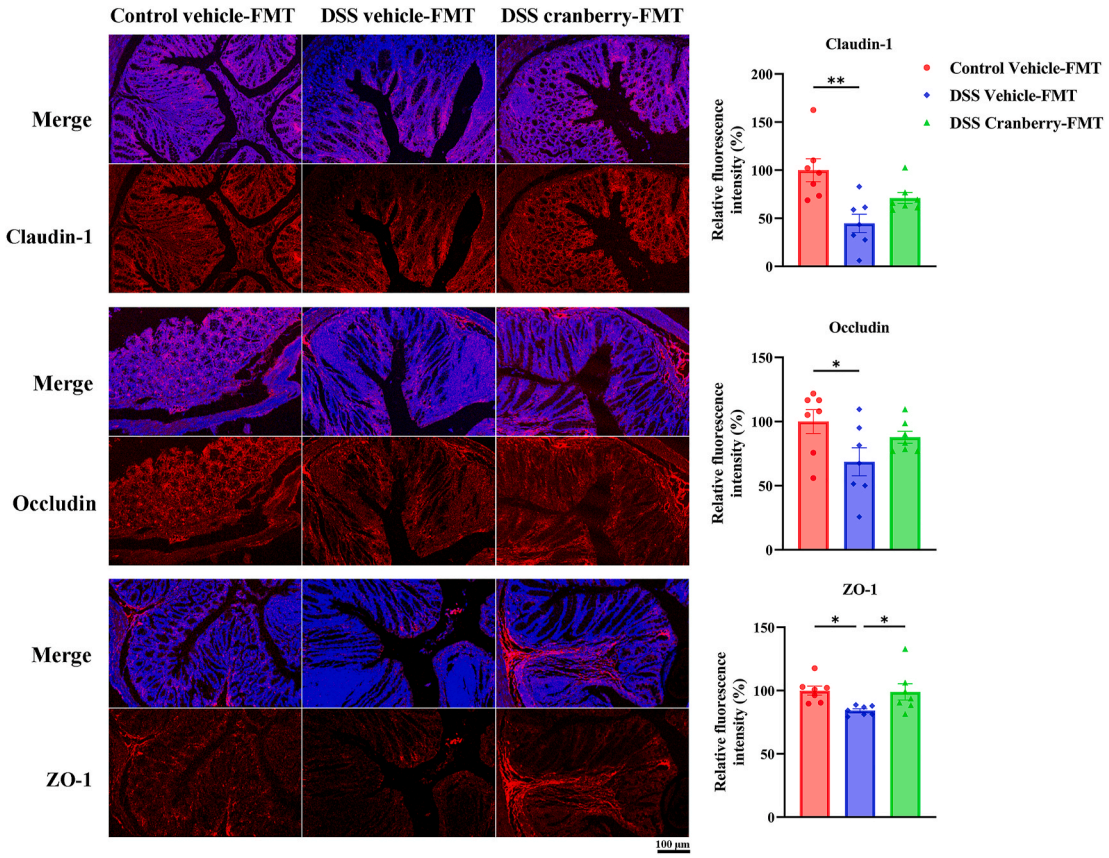

Fig. 14. Tight junction protein levels in colonic samples from cranberry FMT-treated mice. (A) Representative images depicting the expression of claudin-1, occludin, and ZO-1 in the Control Vehicle-FMT, DSS Vehicle-FMT, and DSS Cranberry-FMT groups. Quantitative analysis of fluorescence intensity is shown for (B) claudin-1, (C) occludin, and (D) ZO-1. Cranberry-FMT significantly increased the levels of ZO-1 compared to DSS Vehicle-FMT, whereas claudin-1 and occludin levels did not show a significant increase. Data points represent individual mice, with bar heights indicating the mean ± SEM (n = 7); *p < 0.05, **p < 0.01, ***p < 0.001 indicate statistical differences between groups.

cranberry-FMT group to vehicle-FMT mice, there was no significant increase observed in the majority of SCFAs, including acetic acid, propionic acid, isobutyric acid, valeric acid, and isovaleric acid. From these findings, it can be inferred that cranberry has the potential to moderately enhance SCFA production through the modulation of gut microbiota.

3.12. Cranberry FMT did not maintain intestinal barrier integrity

Finally, the expression of tight junction proteins such as claudin-1, occludin, and ZO-1 was assessed following cranberry-FMT. As shown in Fig. 14, cranberry-FMT did not elevate claudin-1 or occludin levels in IBD mice but did result in increased ZO-1 levels in colonic tissues compared to mice receiving vehicle-FMT. This suggests that cranberry may partially improve intestinal barrier function through the modulation of gut microbiota, specifically by influencing ZO-1 expression.

4. Discussion

Anthocyanins, a class of flavonoids responsible for the vibrant colors of many fruits and vegetables, have been specifically identified as potent anti-inflammatory and antioxidative agents. Their role in IBD treatment has been explored in various preclinical studies, with findings supporting their capacity to modulate inflammatory pathways, reduce oxidative damage, and enhance intestinal barrier integrity (Li et al., 2021; Mo et al., 2022; Mu et al., 2021; Zhang et al., 2022). Our results, showcasing the efficacy of anthocyanin-rich cranberry extract in improving DAI scores, colon length, and colonic morphology, are consistent with the protective effects of anthocyanins reported in the literatures. For example, research on anthocyanin-rich extracts from berries has indicated their ability to downregulate pro-inflammatory cytokines and upregulate antioxidant defense mechanisms (Ortiz et al., 2021; Piberger et al., 2011), similar to the modulation of ferroptosis-associated gene expression and reduction of pro-inflammatory cytokines observed in our study. In addition, the specific impact of anthocyanins on gut microbiota composition, as seen with the cranberry extract in our research, adds to the evidence supporting the prebiotic-like effects of anthocyanins. However, our antibiotic intervention experiment and FMT experiment showed that intestinal flora was not required for the improvement of cranberry extract in IBD treatment. That means that cranberry extract does not modulate intestinal flora directly.

The protective effects of anthocyanins against IBD are primarily mediated through their antioxidant and anti-inflammatory properties. These compounds can scavenge free radicals, reduce oxidative stress, and inhibit pro-inflammatory cytokine production, which are crucial factors in the pathogenesis of IBD. Specifically, in ulcerative colitis, a subtype of IBD characterized by continuous inflammation of the colonic mucosa, the reduction of oxidative stress and inflammation by anthocyanins helps to alleviate mucosal damage and improve clinical symptoms. For instance, anthocyanins have been shown to downregulate pro-inflammatory cytokines such as TNF-α, IL-1β, and IL-6, which play a crucial role in the inflammatory cascade in ulcerative colitis (Breugelmans et al., 2020; Hartman et al., 2016). By suppressing these cytokines, anthocyanins reduce the recruitment of inflammatory cells to the colonic mucosa, thereby mitigating the inflammatory response. Additionally, the enhancement of antioxidant defenses, such as GSH

levels and the upregulation of antioxidant enzymes like GPX4, further protects the colonic tissue from oxidative damage.

Ferroptosis is a form of programmed cell death characterized by iron-dependent lipid peroxidation, and its regulation is crucial in controlling inflammation and cellular damage associated with IBD (Ocansey et al., 2023). The modulation of ferroptosis-related gene expression by cranberry extract, specifically the upregulation of GPX4, SLC7A11, HO-1, and ferritin light chain, has profound implications for colonic health and the pathophysiology of IBD. The upregulation of GPX4 and SLC7A11 contributes to enhancing the antioxidant defense mechanisms within the colonic cells (Li et al., 2022). By increasing the capacity to reduce lipid hydroperoxides and promote glutathione synthesis, cranberry extract effectively reduces oxidative stress, a critical factor in the initiation and progression of IBD. Oxidative damage to cellular components, including lipids, proteins, and DNA, can exacerbate inflammation and disrupt the integrity of the intestinal barrier, leading to the hallmark symptoms of IBD (Alemany-Cosme et al., 2021). Therefore, promoting antioxidant defenses by anthocyanins-rich cranberry extract can help maintain cellular health and prevent the exacerbation of inflammation. The induction of HO-1 and the downregulation of ferritin light chain by cranberry extract play significant roles in regulating iron homeostasis (Smith et al., 2023). Excess free iron can catalyze the formation of reactive oxygen species (ROS) through the Fenton reaction, further contributing to oxidative stress and ferroptosis (Liu et al., 2024). By facilitating the degradation of heme and the storage of iron in a non-reactive form, cranberry extract limits the availability of free iron, thereby reducing oxidative damage and inflammation. These alterations in colonic ferroptosis associated protein suggests the powerful antioxidant action of anthocyanins-rich cranberry extract.

Our study noted a decrease in the relative abundance of pathogenic bacteria such as Proteobacteria and *Escherichia-Shigella*, alongside an increase in beneficial *Lactobacillus* following cranberry extract treatment. This shift towards a more favorable gut microbiota composition is critical in IBD, where dysbiosis, or the imbalance of gut microbiota, plays a critical role in disease pathogenesis (Qiu et al., 2022). The reduction in pathogenic bacteria can lead to decreased intestinal inflammation, as these bacteria often trigger immune responses that exacerbate IBD symptoms. Conversely, the proliferation of *Lactobacillus*, a genus known for its anti-inflammatory and gut barrier-protective effects, can contribute to the maintenance of intestinal homeostasis and the attenuation of IBD symptoms (Dempsey and Corr, 2022). *Lactobacillus* strains have been shown to modulate the host immune response, enhance the mucosal barrier function, and produce metabolites that inhibit pathogens, collectively supporting gut health and potentially counteracting the inflammatory processes characteristic of IBD (Remus et al., 2013; Shen et al., 2024). SCFAs, primarily produced by the fermentation of dietary fibers by gut microbiota, serve as an energy source for colonocytes, strengthen the intestinal barrier, and exert anti-inflammatory effects (Wu et al., 2023; Yan et al., 2024). The observed increase in SCFAs content in our study suggests that cranberry extract may promote the growth of SCFA-producing bacteria, leading to enhanced production of these beneficial metabolites (Ye et al., 2023). SCFAs, particularly butyrate, are crucial for maintaining colonic health (Abdelhalim, 2024). Butyrate not only provides energy for colonocytes but also regulates cell proliferation and differentiation, and induces the production of regulatory T cells, thereby reducing inflammation.

The antibiotic intervention, designed to disrupt the gut microbiota, did not abolish the beneficial effects of cranberry extract on IBD, suggesting that the efficacy of cranberry is not solely dependent on, at least not directly, the presence of a specific microbial community. This finding is critical as it indicates that cranberry extract may exert its therapeutic effects through direct anti-inflammatory and antioxidative pathways, in addition to modulating gut microbiota. However, the attenuation of some benefits post-antibiotic treatment also hints at the contributory role of gut microbiota in fully realizing the therapeutic potential of cranberry extract. This dual mechanism of action, involving both direct effects on the host and indirect effects via microbiota modulation, highlights the complexity of dietary interventions in IBD treatment.

The FMT experiments, wherein microbiota from cranberry-treated donors was transferred to recipient mice, revealed partial effects on IBD-like symptoms and gut health markers (Wang et al., 2023). While the FMT did not significantly decrease IBD-like symptoms to the extent observed with direct cranberry extract treatment, there was a noted increase in SCFAs and partial enhancement of tight junction protein expression. These partial effects suggest that while the transferred gut microbiota retained some beneficial characteristics induced by cranberry extract, such as the capacity to produce SCFAs, not all therapeutic benefits of the extract could be mediated through FMT alone. This discrepancy may be attributed to several factors. First, the complexity of interactions between cranberry-derived anthocyanins and the host gut environment may involve synergistic effects that cannot be fully replicated through FMT. Secondly, the physical and chemical components of cranberry extract, especially anthocyanins, may directly interact with the gut epithelial cells and immune system with its anti-oxidant and anti-inflammatory activities, contributing to its therapeutic effects beyond what can be achieved through microbiota modulation alone. Lastly, the variability in gut microbiota composition between donors and recipients may influence the efficacy of FMT (He et al., 2022), highlighting the personalized nature of microbiota-based interventions. The outcomes of these experiments suggest that while intestinal flora plays a significant role in mediating the effects of cranberry extract on IBD, the benefits of cranberry are not solely dependent on these microbial changes.

In conclusion, our study demonstrates that anthocyanin-rich cranberry extract significantly alleviates symptoms of DSS-induced IBD in mice. The efficacy was involved in the inhibition of ferroptosis and inflammation by cranberry. However, inconsistent with the hypothesis, the antibiotic intervention and FMT revealed that the beneficial effects of cranberry extract are not entirely dependent on the gut microbiota. These finding suggests that anthocyanins-rich cranberry extract attenuates IBD by acting colonic tissue directly but not in an intestinal flora dependent manner.

Data available statement

Data will be made available on request.

CRediT authorship contribution statement

Jun Wang: Investigation, Formal analysis, Writing – original draft. **Zhong-Yu Yuan:** Investigation, Formal analysis. **Xin-Yu Wang:** Investigation, Formal analysis. **Ji-Xiao Zhu:** Investigation, Formal analysis. **Wei-Feng Huang:** Conceptualization. **Guang-Hui Xu:** Conceptualization, Funding acquisition, Supervision, Writing – review & editing. **Li-Tao Yi:** Conceptualization, Funding acquisition, Supervision, Writing – review & editing.

Declaration of competing interest

The authors declare that they have no known competing financial interests or personal relationships that could have appeared to influence the work reported in this paper.

Data availability

Data will be made available on request.

Acknowledgement

This work was supported by Natural Science Foundation of Fujian Province [2022J01315; 2023J011616], Medical and Health Guiding

Project of Xiamen [3502Z20214ZD1028], Xiamen Science and Technology Plan Project [3502Z20226034] and Xiamen Marine and Fishery Development Special Fund [23YYZP013QCA11]. We would like to thank Instrumental Analysis Center of Huaqiao University for the help of confocal testing, and thank Jun Yu from Shiyanjia Lab www.shiyanjia.com for the anthocyanin analysis.

Appendix A. Supplementary data

Supplementary data to this article can be found online at https://doi.org/10.1016/j.crfs.2024.100815.

References

Abdelhalim, K.A., 2024. Short-chain fatty acids (SCFAs) from gastrointestinal disorders, metabolism, epigenetics, central nervous system to cancer - a mini-review. Chem. Biol. Interact. 388, 110851.

Alemany-Cosme, E., Saez-Gonzalez, E., Moret, I., Mateos, B., Iborra, M., Nos, P., Sandoval, J., Beltran, B., 2021. Oxidative stress in the pathogenesis of crohn's disease and the interconnection with immunological response, microbiota, external environmental factors, and epigenetics. Antioxidants 10.

Barnes, J.S., Nguyen, H.P., Shen, S., Schug, K.A., 2009. General method for extraction of blueberry anthocyanins and identification using high performance liquid chromatography-electrospray ionization-ion trap-time of flight-mass spectrometry. J. Chromatogr. A 1216, 4728–4735.

Breugelmans, T., Van Spaendonk, H., De Man, J.G., De Schepper, H.U., Jauregui-Amezaga, A., Macken, E., Linden, S.K., Pintelon, I., Timmermans, J.P., De Winter, B. Y., Smet, A., 2020. In-depth study of transmembrane mucins in association with intestinal barrier dysfunction during the course of T cell transfer and DSS-induced colitis. J Crohns Colitis 14, 974–994.

Cai, X., Han, Y., Gu, M., Song, M., Wu, X., Li, Z., Li, F., Goulette, T., Xiao, H., 2019. Dietary cranberry suppressed colonic inflammation and alleviated gut microbiota dysbiosis in dextran sodium sulfate-treated mice. Food Funct. 10, 6331–6341.

Cheng, J., Liu, D., Huang, Y., Chen, L., Li, Y., Yang, Z., Fu, S., Hu, G., 2023. Phlorizin mitigates dextran sulfate sodium-induced colitis in mice by modulating gut microbiota and inhibiting ferroptosis. J. Agric. Food Chem. 71, 16043–16056.

Dempsey, E., Corr, S.C., 2022. Lactobacillus spp. for gastrointestinal health: current and future perspectives. Front. Immunol. 13, 840245.

Feldman, F., Koudoufio, M., El-Jalbout, R., Sauve, M.F., Ahmarani, L., Sane, A.T., Ould-Chikh, N.E., N'Timbane, T., Patey, N., Desjardins, Y., Stintzi, A., Spahis, S., Levy, E., 2022. Cranberry proanthocyanidins as a therapeutic strategy to curb metabolic syndrome and fatty liver-associated disorders. Antioxidants 12.

Gao, T., Hou, M., Zhang, B., Pan, X., Liu, C., Sun, C., Jia, M., Lin, S., Xiong, K., Ma, A., 2021. Effects of cranberry beverages on oxidative stress and gut microbiota in subjects with Helicobacter pylori infection: a randomized, double-blind, placebo-controlled trial. Food Funct. 12, 6878–6888.

Glauser, G., Grund, B., Gassner, A.L., Menin, L., Henry, H., Bromirski, M., Schutz, F., McMullen, J., Rochat, B., 2016. Validation of the mass-extraction-window for quantitative methods using liquid chromatography high resolution mass spectrometry. Anal. Chem. 88, 3264–3271.

Glisan, S.L., Ryan, C., Neilson, A.P., Lambert, J.D., 2016. Cranberry extract attenuates hepatic inflammation in high-fat-fed obese mice. J. Nutr. Biochem. 37, 60–66.

Gunathilake, M., Lee, J., Choi, I.J., Kim, Y.I., Yoon, J., Sul, W.J., Kim, J.F., Kim, J., 2020. Alterations in gastric microbial communities are associated with risk of gastric cancer in a Korean population: a case-control study. Cancers 12.

Hartman, D.S., Tracey, D.E., Lemos, B.R., Erlich, E.C., Burton, R.E., Keane, D.M., Patel, R., Kim, S., Bhol, K.C., Harris, M.S., Fox, B.S., 2016. Effects of AVX-470, an oral, locally acting anti-tumour necrosis factor antibody, on tissue biomarkers in patients with active ulcerative colitis. J Crohns Colitis 10, 641–649.

He, R., Li, P., Wang, J., Cui, B., Zhang, F., Zhao, F., 2022. The interplay of gut microbiota between donors and recipients determines the efficacy of fecal microbiota transplantation. Gut Microb. 14, 2100197.

Heiss, C., Istas, G., Feliciano, R.P., Weber, T., Wang, B., Favari, C., Mena, P., Del Rio, D., Rodriguez-Mateos, A., 2022. Daily consumption of cranberry improves endothelial function in healthy adults: a double blind randomized controlled trial. Food Funct. 13, 3812–3824.

Li, F.J., Long, H.Z., Zhou, Z.W., Luo, H.Y., Xu, S.G., Gao, L.C., 2022. System X(c) (-)/GSH/GPX4 axis: an important antioxidant system for the ferroptosis in drug-resistant solid tumor therapy. Front. Pharmacol. 13, 910292.

Li, S., Wang, T., Wu, B., Fu, W., Xu, B., Pamuru, R.R., Kennett, M., Vanamala, J.K.P., Reddivari, L., 2021. Anthocyanin-containing purple potatoes ameliorate DSS-induced colitis in mice. J. Nutr. Biochem. 93, 108616.

Liu, J., Hao, W., He, Z., Kwek, E., Zhu, H., Ma, N., Ma, K.Y., Chen, Z.Y., 2021. Blueberry and cranberry anthocyanin extracts reduce bodyweight and modulate gut microbiota in C57BL/6 J mice fed with a high-fat diet. Eur. J. Nutr. 60, 2735–2746.

Liu, Y., Hu, S., Shi, B., Yu, B., Luo, W., Peng, S., Du, X., 2024. The role of iron metabolism in sepsis-associated encephalopathy: a potential target. Mol. Neurobiol. 61, 4677–4690.

Mo, J., Ni, J., Zhang, M., Xu, Y., Li, Y., Karim, N., Chen, W., 2022. Mulberry anthocyanins ameliorate DSS-induced ulcerative colitis by improving intestinal barrier function and modulating gut microbiota. Antioxidants 11.

Mu, J., Xu, J., Wang, L., Chen, C., Chen, P., 2021. Anti-inflammatory effects of purple sweet potato anthocyanin extract in DSS-induced colitis: modulation of commensal bacteria and attenuated bacterial intestinal infection. Food Funct. 12, 11503–11514.

Ocansey, D.K.W., Yuan, J., Wei, Z., Mao, F., Zhang, Z., 2023. Role of ferroptosis in the pathogenesis and as a therapeutic target of inflammatory bowel disease. Int. J. Mol. Med. 51 submitted for publication.

Ortiz, T., Arguelles-Arias, F., Begines, B., Garcia-Montes, J.M., Pereira, A., Victoriano, M., Vazquez-Roman, V., Perez Bernal, J.L., Callejon, R.M., De-Miguel, M., Alcudia, A., 2021. Native Chilean berries preservation and in vitro studies of a polyphenol highly antioxidant extract from maqui as a potential agent against inflammatory diseases. Antioxidants 10.

Perler, B.K., Ungaro, R., Baird, G., Mallette, M., Bright, R., Shah, S., Shapiro, J., Sands, B. E., 2019. Presenting symptoms in inflammatory bowel disease: descriptive analysis of a community-based inception cohort. BMC Gastroenterol. 19, 47.

Piberger, H., Oehme, A., Hofmann, C., Dreiseitel, A., Sand, P.G., Obermeier, F., Schoelmerich, J., Schreier, P., Krammer, G., Rogler, G., 2011. Bilberries and their anthocyanins ameliorate experimental colitis. Mol. Nutr. Food Res. 55, 1724–1729.

Qiu, P., Ishimoto, T., Fu, L., Zhang, J., Zhang, Z., Liu, Y., 2022. The gut microbiota in inflammatory bowel disease. Front. Cell. Infect. Microbiol. 12, 733992.

Ramos, G.P., Papadakis, K.A., 2019. Mechanisms of disease: inflammatory bowel diseases. Mayo Clin. Proc. 94, 155–165.

Remus, D.M., Bongers, R.S., Meijerink, M., Fusetti, F., Poolman, B., de Vos, P., Wells, J. M., Kleerebezem, M., Bron, P.A., 2013. Impact of Lactobacillus plantarum sortase on target protein sorting, gastrointestinal persistence, and host immune response modulation. J. Bacteriol. 195, 502–509.

Salmasi, K., Hassanpour, A., Amouoghli Tabrizi, B., Moghaddam, S., 2023. The role of alcohol extract of cranberry in improving serum indices of experimental metaproterenol-induced heart damage in rats. Food Sci. Nutr. 11, 6670–6675.

Sergazy, S., Shulgau, Z., Kamyshanskiy, Y., Zhumadilov, Z., Krivyh, E., Gulyayev, A., Aljofan, M., 2023. Blueberry and cranberry extracts mitigate CCL4-induced liver damage, suppressing liver fibrosis, inflammation and oxidative stress. Heliyon 9, e15370.

Shen, M., Shi, Y., Ge, Z., Qian, J., 2024. Effects of mesalamine combined with live combined bifidobacterium, Lactobacillus and Enterococcus capsules on intestinal mucosa barrier function and intestinal microbiota in mildly active crohn's disease patients. J. Invest. Surg. 37, 2297565.

Smith, M.J., Yang, F., Griffiths, A., Morrell, A., Chapple, S.J., Siow, R.C.M., Stewart, T., Maret, W., Mann, G.E., 2023. Redox and metal profiles in human coronary endothelial and smooth muscle cells under hyperoxia, physiological normoxia and hypoxia: effects of NRF2 signaling on intracellular zinc. Redox Biol. 62, 102712.

Wang, L., Zhang, P., Chen, J., Li, C., Tian, Y., Xu, F., 2023. Prebiotic properties of the polysaccharide from Rosa roxburghii Tratt fruit and its protective effects in high-fat diet-induced intestinal barrier dysfunction: a fecal microbiota transplantation study. Food Res. Int. 164, 112400.

Wu, X., Xue, L., Tata, A., Song, M., Neto, C.C., Xiao, H., 2020. Bioactive components of polyphenol-rich and non-polyphenol-rich cranberry fruit extracts and their chemopreventive effects on colitis-associated colon cancer. J. Agric. Food Chem. 68, 6845–6853.

Wu, Y., Guo, Y., Huang, T., Huang, D., Liu, L., Shen, C., Jiang, C., Wang, Z., Chen, H., Liang, P., Hu, Y., Zheng, Z., Liang, T., Zhai, D., Zhu, H., Liu, Q., 2023a. Licorice flavonoid alleviates gastric ulcers by producing changes in gut microbiota and promoting mucus cell regeneration. Biomed. Pharmacother. 169, 115868.

Wu, Y., Ran, L., Yang, Y., Gao, X., Peng, M., Liu, S., Sun, L., Wan, J., Wang, Y., Yang, K., Yin, M., Chunyu, W., 2023b. Deferasirox alleviates DSS-induced ulcerative colitis in mice by inhibiting ferroptosis and improving intestinal microbiota. Life Sci. 314, 121312.

Xu, S., He, Y., Lin, L., Chen, P., Chen, M., Zhang, S., 2021. The emerging role of ferroptosis in intestinal disease. Cell Death Dis. 12, 289.

Yan, W., Luo, J., Yu, Z., Xu, B., 2024. A critical review on intestinal mucosal barrier protection effects of dietary polysaccharides. Food Funct. 15, 481–492.

Yang, Y., Lv, L., Shi, S., Cai, G., Yu, L., Xu, S., Zhu, T., Su, X., Mao, N., Zhang, Y., Peng, S., He, J., Liu, Z., Wang, D., 2023. Polysaccharide from walnut green husk alleviates liver inflammation and gluconeogenesis dysfunction by altering gut microbiota in ochratoxin A-induced mice. Carbohydr. Polym. 322, 121362.

Ye, J., Li, Y., Wang, X., Yu, M., Liu, X., Zhang, H., Meng, Q., Majeed, U., Jian, L., Song, W., Xue, W., Luo, Y., Yue, T., 2023. Positive interactions among Corynebacterium glutamicum and keystone bacteria producing SCFAs benefited T2D mice to rebuild gut eubiosis. Food Res. Int. 172, 113163.

Zhang, G., Gu, Y., Dai, X., 2022. Protective effect of bilberry anthocyanin extracts on dextran sulfate sodium-induced intestinal damage in Drosophila melanogaster. Nutrients 14.